This is a repository copy of *The dynamin-related protein Vps1 and the peroxisomal membrane protein Pex27 function together during peroxisome fission*.

White Rose Research Online URL for this paper:
https://eprints.whiterose.ac.uk/197747/

Version: Published Version

Article:

The dynamin-related protein Vps1 and the peroxisomal membrane protein Pex27 function together during peroxisome fission

Lakhan Ekal[*], Abdulaziz MS Alqahtani and Ewald H. Hettema[‡]

Department of Molecular Biology and Biotechnology, University of Sheffield, Sheffield, UK

*Present address: European Molecular Biology Laboratory, Hamburg, Germany

[‡]Corresponding author: e.hettema@sheffield.ac.uk

Summary statement

Yeast peroxisome fission is mediated by the dynamin-related proteins Vps1 and Dnm1. Pex27 accumulates at peroxisomal membrane constrictions and is specifically required for Vps1 accumulation and or activity on peroxisomes.

ABSTRACT

Dynamin-related proteins (Drp) mediate a variety of membrane remodelling processes. The fungal Drp, Vps1, is required for endocytosis, endosomal sorting, vacuole fusion and peroxisome fission and breakdown. How Drps, and in particular Vps1, can mediate their function at so many different subcellular locations is of interest to our understanding of cellular organisation. We found that the peroxisomal membrane protein Pex27 is specifically required for Vps1-dependent peroxisome fission in proliferating cells but is not required for Dnm1-dependent peroxisome fission. Pex27 accumulates in constricted regions of peroxisomes and affects peroxisome geometry upon overexpression. Moreover, Pex27 physically interacts

with Vps1 *in vivo* and is required for accumulation of a GTPase defective Vps1 mutant (K42A), on peroxisomes. During nitrogen starvation, a condition that halts cell division and induces peroxisome breakdown, Vps1 associates with the pexophagophore. Pex27 is neither required for Vps1 recruitment to the pexophagophore nor for pexophagy. Our study identifies Pex27 as a Vps1 specific partner for the maintenance of peroxisome number in proliferating yeast cells.

INTRODUCTION

Dynamin-related proteins (Drps) comprise a group of self-assembling GTPases that mediate intracellular membrane fission and fusion events. Their activities affect processes such as endocytosis, endosomal protein sorting, organelle fission and fusion (Ferguson and De Camilli, 2012; Praefcke and McMahon, 2004). Drps contain conserved functional domains including a large GTPase domain. In addition, the founding member of this protein family, dynamin, contains a pleckstrin homology domain (PHD) and a proline rich domain (PRD) that are required for lipid binding and for interaction with other proteins, respectively (Jimah and Hinshaw, 2019).

Dynamin's best studied function is in clathrin mediated endocytosis (CME) where it induces scission of endocytic vesicles from the plasma membrane. *In vitro* studies show that dynamin assembles onto tubulated membranes to form helical polymers that constrict upon GTP binding and further constrict upon GTP hydrolysis to induce fission; for review see (Antonny et al., 2016). A variety of proteins interact with dynamin at sites of CME. These proteins act as adaptors to specifically recruit dynamin and or regulate its activity. Among these proteins, the bar domain-containing proteins amphiphysin and endophilin generate membrane curvature at the vesicle neck, which allows dynamin polymers to assemble (Ross et al., 2011; Roux et al., 2010; Takei et al., 1999).

Drp1 (Dnm1 in *Saccharomyces cerevisiae*) is required for fission of intracellular organelles such as mitochondria and peroxisomes; for review see (Jimah and Hinshaw, 2019). In *S. cerevisiae* a second Drp, Vps1, is involved in peroxisome fission (Hoepfner et al., 2001). Vps1 is also involved in endocytosis (Smaczynska-de et al., 2010), multiple endosomal trafficking events (Lukehart et al., 2013; Nothwehr et al., 1995; Wilsbach and Payne, 1993), peroxisome breakdown (Mao et al., 2014)

and vacuole fusion (Peters et al., 2004). Although related to dynamin, it lacks a PHD and PRD. Instead it contains a region that varies among the Drps, called insert B (Varlakhanova et al., 2018). Insert B of Vps1 has been proposed to functionally resembling the PHD of dynamin (Smaczynska-de et al., 2019). As described for dynamin, Vps1 assembles on lipid nanotubes *in vitro* and interacts with membrane curvature inducing proteins such as amphiphysin (Rvs167) and the bar domain containing sorting nexin Mvp1, *in vivo* (Chi et al., 2014; Ma et al., 2017; Smaczynska-de et al., 2012). Mvp1 has been shown to tubulate endosomal membranes and recruit Vps1 to sites of fission (Suzuki et al., 2021). There is a longstanding interest in the identification of factors that contribute to dynamin and Drp-dependent functions in order to fully understand how these proteins execute a wide variety of functions on different target membranes, including the peroxisomal membrane.

Vps1 is the main Drp that mediates peroxisome fission in dividing *S. cerevisiae* cells, with only a minor contribution of Dnm1 (Hoepfner et al., 2001; Kuravi et al., 2006; Motley and Hettema, 2007). Dnm1 dependent peroxisome fission relies on the cofactors Fis1, Mdv1 and Caf4, that recruit and regulate Dnm1 activity. The Dnm1 cofactors are not required for Vps1 dependent peroxisome fission (Motley et al., 2008). When peroxisomes are no longer required, especially under conditions of nitrogen starvation, they are removed by pexophagy (Hutchins et al., 1999). The peroxisomal membrane protein Pex3 recruits the pexophagy receptor Atg36. Atg36 connects peroxisomes via Atg11 and Atg8 with the core autophagy machinery (Motley et al., 2012a; Motley et al., 2012b). Efficient pexophagy relies on fission of peroxisomes into small portions to allow incorporation into pexophagosomes. Under these conditions, Atg36 and Atg11 are both required to recruit Vps1 to peroxisomes (Mao et al., 2014). Peroxisome number is not reduced in proliferating cells lacking Atg11 or Atg36 (Motley et al., 2012b). This raises the question how Vps1 activity on peroxisomal membranes is achieved in proliferating cells as it seems unlikely that Atg11 and Atg36 are required.

Peroxisomes divide by a multistep process that comprises membrane elongation, constriction and fission. Candidate proteins that may contribute to Vps1-dependent peroxisome fission are the Pex11 family of peroxisomal membrane proteins. This family of proteins is conserved among eukaryotes and has been linked to

peroxisome division (Honsho et al., 2016; Schrader et al., 2016) and some family members have been implicated in *de novo* formation of peroxisomes (Chang et al., 2015; Huber et al., 2012). In addition, Pex11 family members have been assigned roles in peroxisomal metabolism and membrane contact site with other organelles; for review see (Carmichael and Schrader, 2022). Loss of Pex11β function in humans leads to disease (Ebberink et al., 2012). Phylogenetic analysis revealed a complex evolutionary history of the Pex11 family; for overview see (Chang et al., 2015; Jansen et al., 2021). Several members of the Pex11 family, including Pex11β, contain an amphipathic helix that is required for membrane remodelling activity *in vitro* and peroxisome fission *in vivo* (Opalinski et al., 2011; Su et al., 2018; Yoshida et al., 2015). Pex11 oligomerisation is also important for membrane remodelling and is considered important for membrane tubulation and assembly of the fission machinery (Bonekamp et al., 2013; Itoyama et al., 2012). Pex11β in mammals and Pex11 in *Hansenula polymorpha* interact with Fis1 and Drp1/Dnm1 which is thought to couple membrane remodelling and Dnm1 recruitment. In addition, Pex11β/Pex11 physically interacts with Drp1/Dnm1 directly and stimulates its GTPase activity (Schrader et al., 2022; Williams et al., 2015).

In *S. cerevisiae*, the Pex11 family consists of Pex11, Pex25 and Pex27. ScPex11 is required for peroxisome proliferation in response to growth on fatty acids such as oleate as sole carbon source (Erdmann and Blobel, 1995; Marshall et al., 1995) for fatty acid β-oxidation (Mindthoff et al., 2016; van Roermund et al., 2000) and it mediates contacts between mitochondria and peroxisomes (Esposito et al., 2019; Mattiazzi Usaj et al., 2015). Pex25 is a fungal innovation (Chang et al., 2015). Its paralogue Pex27 is thought to have subsequently arisen during the whole genome duplication of an ancestor of *S. cerevisiae* (Byrne and Wolfe, 2005) and is found in a subset of yeasts only. Both proteins affect peroxisome number and shape during peroxisome proliferation but also under non-proliferation inducing conditions (growth on glucose containing media) (Rottensteiner et al., 2003; Smith et al., 2002; Tam et al., 2003; Tower et al., 2011). A population of exponential phase growing *pex25Δ* cells display multiple defects, including cells with a low number of enlarged peroxisomes, partial mislocalisation of matrix proteins to the cytosol, segregation defects. This segregation defect would normally induce *de novo* peroxisome formation but this process is strongly delayed in *pex25Δ* cells, thereby resulting in

cells lacking peroxisomal structures altogether (Huber et al., 2012; Rottensteiner et al., 2003; Smith et al., 2002; Tam et al., 2003). The molecular role of Pex25 in peroxisome dynamics remains unclear but Pex25 has been shown to initiate elongation and tubulation of the peroxisomal membrane which has been proposed to be required for both Vps1-dependent and Dnm1-dependent peroxisome fission (Huber et al., 2012). Pex27 is a low expressed and poorly characterised member of the Pex11 family of proteins. Pex27 is constitutively expressed whereas Pex11 and Pex25 are further induced on oleate media. *PEX27* gene deletion reduces peroxisome number (Rottensteiner et al., 2003; Tam et al., 2003; Tower et al., 2011) and Pex27 overexpression has been reported to antagonise Pex25 function (Huber et al., 2012). Pex34 is a distantly related to the Pex11 protein family that regulates peroxisome number in concert with Pex11 family proteins (Jansen et al., 2021; Tower et al., 2011).

Here we report that Pex27 is specifically required for Vps1-dependent peroxisome fission in dividing cells but not for Dnm1-dependent peroxisome fission. We found that Pex27 can physically interact with Vps1 and that accumulation of the Vps1 GTPase deficient mutant Vps1-K42A-GFP on peroxisomes is dependent on Pex27. In a peroxisome fission deficient mutant, Pex27-mNG localises to constricted sites on the peroxisomal membrane. Overexpression of Pex27 induces an increase in peroxisome number in the presence of Vps1 but in *vps1Δ/dnm1Δ* cells, Pex27 overexpression induces narrow tubules that connect bulbous parts of the peroxisomal structures, resulting in dumbbell-shaped peroxisomes. It is on these tubular connections that Pex27-mNG accumulates. Our data support a model whereby Pex27 recruits Vps1 or facilitates assembly of Vps1 oligomers to constricted sites on the peroxisomal membrane. In addition, we found that Pex27 is not required for pexophagy and recruitment of Vps1 to peroxisomes under pexophagy conditions. This qualifies Pex27 as a conditional cofactor of Vps1 on peroxisomes.

RESULTS

Pex27 is required for Vps1-dependent peroxisome fission

In most organisms studied, peroxisome fission relies on a single DRP, Dnm1/Drp1. Fungal Dnm1/Drp1 acts in concert with Fis1, Mdv1 and as shown in *H. polymorpha*, also Pex11. Peroxisome fission in *S. cerevisiae*, mainly relies on the Drp, Vps1, and to a lesser extent, Dnm1. As Vps1 dependent fission is not dependent upon Fis1, Mdv1, and its paralogue Caf4 (Motley et al., 2008; Nagotu et al., 2008) we set out to identify factors specifically required for Vps1-dependent peroxisome fission. We generated double gene deletion mutants of *PEX11*, *PEX25*, *PEX27*, and *PEX34* with either a *VPS1* or a *DNM1* deletion and expressed monomeric Neon Green (mNG) fluorescent protein appended with a peroxisome targeting signal type 1 (PTS1) in them that allows for bright labelling of peroxisomes in living cells and compared peroxisome number in each of these strains. A factor specifically required for Vps1-dependent fission is expected to 1) show a strong decrease in peroxisome number when deleted on its own, as is observed in *vps1Δ* cells, 2) have no further decrease in peroxisome number upon *VPS1* deletion and 3) show a further decrease in peroxisome number upon *DNM1* deletion. We standardised our growth conditions so that we were only analysing cells in the exponential growth phase on glucose medium (see materials and methods). An initial screen revealed that only one mutant, *pex27Δ*, fitted our criteria (Fig. S1). A selection of strains was regrown making sure that overnight cultures did not reach stationary phase before dilution in the morning and at least 6 hr growth in fresh glucose medium. Deletion of *PEX27* results in a strong reduction in peroxisome number, that is further significantly reduced in *pex27Δ/dnm1Δ* cells but not in *vps1Δ/pex27Δ* cells (Fig. 1A). The peroxisomes in *pex27Δ/dnm1Δ* cells are mostly elongated, frequently extending from the mother cell into the bud. This phenotype is also observed in *vps1Δ/dnm1Δ* cells (Fig. 1A,S1). These observations suggest that Pex27 and Vps1 may operate together in the maintenance of peroxisome number.

We used a previously developed mating approach that specifically assays for Vps1-dependent peroxisome fission (Motley et al., 2007) to test for the requirement of Pex27. Haploid *vps1Δ/dnm1Δ* cells pulse labelled with mNeonGreen (mNG)-PTS1 were mated with MatA *pex3Δ* cells expressing mKate2-PTS1. *pex3Δ* cells are devoid

of typical peroxisomal membrane structures and many PMPs are present at low level (Hettema et al., 2000; Wroblewska et al., 2017) including Pex27 (Fig. 1C). In this assay, Vps1 from the MatA *pex3Δ* cell diffuses into the Matα *vps1Δ/dnm1Δ* cell and remodels and divides the single pre-labelled peroxisome into multiple smaller ones (Fig. 1B, panel I,II,III and IV). Remodelling occurs rapidly upon mating, before the cytosolic mKate2-PTS1 pool becomes evidently punctate (Fig. 1B panel I). By the time zygotes are formed, all (18/18 zygotes) showed multiple dispersed peroxisomes. Dnm1 does not contribute to peroxisome fission under these assay conditions, probably as it is mainly associated with mitochondria and no free pool of Dnm1 is available (Motley and Hettema, 2007; Motley et al., 2008). Indeed, if MatA *pex3Δ* cells additionally lack *VPS1*, peroxisomes do not divide upon mating and zygotes contain a single peroxisomal structure (15/15 zygotes) (Fig.1B, panel V, see also (Motley and Hettema, 2007)). In Matα *vps1Δ/dnm1Δ* cells lacking *PEX27*, reintroduction of Vps1 upon mating with MatA *pex3Δ* cells does not rescue peroxisome fission before import of mKate2-PTS1 is observed. Even at later stages of mating, when mKate2-PTS1 was clearly imported and zygotes were being formed, we observed elongated peroxisomes in all cells (Fig. 1B panel V,VI,VII), with 11 out of 15 zygotes containing 1 or 2 peroxisomal structures. The remaining 4 zygotes contained a low number of puncta and elongated peroxisomes (Fig. 1B, panel VIII), suggesting that fission started to be restored. The observation that fission is being restored in large zygotes is not completely unexpected as newly synthesised Pex27 will now be routed to the Pex27-deficient pre-existing peroxisome. We conclude, Vps1-dependent peroxisome fission requires Pex27. Vps1 is involved in many membrane remodelling events including protein sorting through the endomembrane system (Lukehart et al., 2013; Nothwehr et al., 1995; Wilsbach and Payne, 1993). The steady state distribution of GFP-Snc1 is a good marker for recycling through the endosomal system (Lewis et al., 2000). This v-SNARE is required for fusion of secretory vesicles with the plasma membrane and is recycled via endosomes to the late Golgi. As secretion is a polarised process in *S. cerevisiae*, GFP-Snc1 strongly labels the plasma membrane in buds and in the bud neck in cells prior to cytokinesis (Lewis et al., 2000). In *vps1Δ* cells, GFP-Snc1 is not retrieved from endosomes but instead accumulates in the vacuole (Ma et al., 2017). GFP-Snc1 steady state distribution is unaffected in *pex27Δ* cells (Fig. 1D). These results strongly suggest that Pex27 is a factor specifically required for Vps1-dependent peroxisome

multiplication, which is in agreement with its localisation at the peroxisomal membrane (Rottensteiner et al., 2003; Tam et al., 2003).

Pex27 level is limiting Vps1-dependent peroxisome fission

Overexpression of Dnm1 but not Vps1 restores peroxisome abundance in *pex27Δ* and *dnm1Δ/pex27Δ* cells (Fig. 2A). This corroborates the model that Pex27 is specifically required for Vps1-dependent peroxisome fission. Although overexpression of Vps1 restores peroxisome number in *vps1Δ/dnm1Δ* cells, it does not induce an increase in peroxisome number in wild type (WT) cells (Fig. 2B,C, S2A). This suggests that Vps1 is not limiting for peroxisome fission. Overexpression of Pex27 has previously been reported to interfere with peroxisome functioning by antagonising Pex25 activity (Huber et al., 2012). Indeed, Pex27 overexpression resulted in partial mislocalisation of a peroxisomal matrix marker in some cells, thereby somewhat resembling *pex25Δ* cells (Fig. S3A). However, when using the peroxisomal membrane proteins Pex11-mNG and Pex13-GFP as markers, we found an increase in peroxisomal membrane structures upon Pex27 overexpression that was dependent upon Vps1 (Fig. 2B,C and S3B,C). This Pex27 overexpression phenotype is different from *pex25Δ* cells as in *pex25Δ* cells Pex11-mNG is either localised to the low number of peroxisomes or mislocalised to tubular network most likely to be mitochondria (Fig. S3D). Pex11 has previously been shown to mistarget to mitochondria in cells that lack peroxisomal membrane structures (Motley et al., 2015). How Pex27 overexpression interferes with matrix protein import is unclear but as it is unrelated to excessive fission of peroxisomes this was not further investigated. We conclude that the level of Pex27 is limiting for Vps1-dependent peroxisome fission.

Epistatic analysis suggests that Pex25 acts upstream of Pex27, Vps1 and Dnm1 as *pex25Δ*/*pex27Δ* and *pex25Δ*/*vps1Δ/dnm1Δ* display a phenotype similar to *pex25Δ* cells e.g. cells are either lacking peroxisomes or contain a reduced number of spherical peroxisomes with many cells showing partial mislocalisation of matrix proteins (Fig. 2D and S1). Overexpression of *VPS1* or *DNM1* does not restore peroxisome number in *pex25Δ* cells (Fig. S2B). Whereas many *pex27Δ*, *vps1Δ* and *vps1Δ/dnm1Δ* mutants display tubular peroxisomes, tubular peroxisomes are mostly

absent when *PEX25* is deleted in these mutants (Fig. 2D and S3H,I). This is in agreement with previous studies that proposed a role for Pex25 in peroxisome tubulation (Huber et al., 2012). Although those *pex25Δ* cells that contain peroxisomes localise Pex27-mNG to peroxisomes (Fig. S3F), overexpression of *PEX27* does not induce peroxisome tubulation or multiplication in *pex25Δ* cells and *vps1Δ/dnm1Δ/pex25Δ* (Fig. S3D,E,H,I). Therefore, we conclude that Pex27 activity is dependent upon Pex25.

Vps1 accumulation on peroxisomes requires Pex27

To analyse localisation of Vps1 to peroxisomes, we expressed Vps1-GFP from a plasmid in *vps1Δ/dnm1Δ* cells controlled by its own promoter. Vps1-GFP rescues peroxisome fission (Fig. 3A) but no convincing colocalization with peroxisomes was observed. The lack of Vps1-GFP localisation to peroxisomes may be a consequence of Vps1 being present briefly during a fission event as has been reported for the scission of endocytic vesicles from the plasma membrane (<10 s) (Smaczynska-de et al., 2010). To visualise Vps1 on peroxisomes we used a GTPase defective mutant (Vps1-K42A) that locks the protein in a constricted helical assembly on its membrane substrate (Sundborger et al., 2014; Tornabene et al., 2020; Varlakhanova et al., 2018). This mutant does not restore peroxisome fission in *vps1Δ/dnm1Δ* cells (Fig. 3A,B). Vps1-K42A-GFP is mainly localised to endosomal structures (Tornabene et al., 2020; Varlakhanova et al., 2018) but we also observed colocalisation of GFP signal with peroxisomes (Fig. 3B). Vps1-K42A-GFP did not label the peroxisomal structure completely but a punctate pattern was observed along the length of the elongated peroxisome (Fig. 3B). In *vps1Δ/dnm1Δ/pex27Δ* cells, Vps1-K42A-GFP no longer decorated the elongated peroxisomes (Fig. 3C). This suggests that Pex27 plays a specific role in Vps1 recruitment or assembly onto peroxisomal membranes. A Pex27-TAP tagged strain (Ghaemmaghami et al., 2003) was transformed with a centromeric plasmid encoding Vps1-GFP under control of its endogenous promoter and as negative control, a plasmid encoding GFP-PTS1 under control of the strong constitutive *TPI1* promoter. Using GFP-TRAP, GFP-PTS1 and Vps1-GFP were precipitated. Pex27-TAP and endogenous Vps1 co-precipitated with Vps1-GFP but

not with GFP-PTS1. This indicates that Pex27 and Vps1 can physically interact *in vivo* and that Vps1-GFP assembles into Vps1 oligomers (Fig. 3D).

Pex27 localises to punctate structures along the peroxisomal membrane in *vps1Δ/dnm1Δ* cells

We C-terminally tagged Pex27 with mNG at its endogenous genomic locus. In WT cells, Pex27-mNG localises to peroxisomes (Fig. 4A). Interestingly, Pex27-mNG does not label the complete peroxisome in mutants with enlarged tubular peroxisomes (*vps1Δ* and *vps1Δ/dnm1Δ* cells) as it appears to be absent from the bulbous parts containing matrix proteins (Fig. 4A). This is in contrast to Pex11-mNG that showed a complete overlap with the HcRed-PTS1 marker in *vps1Δ/dnm1Δ* cells (Fig. 4B). In *vps1Δ* and *vps1Δ/dnm1Δ* cells, peroxisomes form single elongated peroxisomes that consists of a chain of small peroxisomes connected via short constrictions (Hoepfner et al., 2001; Kuravi et al., 2006). As the resolution of epifluorescence microscopy is too low to clearly document sub-peroxisomal protein distribution, we resorted to structured illumination microscopy (SIM) using Pex11-mNG as membrane marker and HcRed-PTS1 as the peroxisomal matrix marker. As expected, Pex11-mNG labels the membrane of vesicles that are part of a single structure. The vesicle lumen labels with HcRed-PTS1 (Fig. 4C). On the other hand, Pex27-mNG displays a string of puncta. These puncta are present between puncta of the matrix marker (Fig. 4D). This indicates that Pex27 accumulates at sites of membrane constriction. Upon overexpression of untagged Pex27 in *vps1Δ/dnm1Δ* cells, peroxisome morphology changed from a tubular structure that was labelled throughout with both matrix and membrane marker to either bulbous peroxisomes with very weakly labelled long extensions or dumbbell-shaped peroxisome with very weakly labelled connecting tubules (Fig. 4E). These elongated tubules are absent in *vps1Δ/dnm1Δ/pex25Δ* cells overexpressing Pex27 (Fig. S3I) although some short extensions were observed in a low percentage of cells (<2% of peroxisomes containing cells) (Fig S3I). Upon overexpression of Pex27-GFP in *vps1Δ/dnm1Δ* cells, the tubular extensions between the bulbous part of the peroxisomes labelled with Pex27-GFP whereas the bulbous parts were devoid of Pex27-GFP (Fig. 4F). The tubular connections between the bulbous parts showed again very weak luminal

staining. Although the overexpression of Pex27 appears to induce or extend narrow peroxisomal membrane tubules, peroxisomal membrane structures in *vps1Δ/dnm1Δ/pex27Δ* cells are still showing constricted areas (Fig. 4G,H), indicating that membrane constriction does not require Pex27. In the few *vps1Δ/dnm1Δ/pex25Δ* cells overexpressing Pex27-GFP that contain short elongated peroxisomes, Pex27-GFP was concentrated on the tubular part of these peroxisomes (Fig. S3J). This indicates Pex27 does not require Pex25 for association with tubular parts of the peroxisomal membrane.

Atg36 is not required for Vps1-dependent peroxisome multiplication in proliferating cells

During starvation, peroxisomes are degraded by pexophagy. Efficient incorporation into pexophagophores requires peroxisomes to be divided by Vps1. Vps1 recruitment to the pexphagophore requires the pexophagy receptor Atg36 and the adapter Atg11 (Liu et al., 2018; Mao et al., 2014). However, peroxisomes abundance in proliferating *atg36Δ* and *atg11Δ* cells is unaffected (Motley et al., 2012b) (Fig. 5A,C), suggesting that Vps1-dependent peroxisome fission under this condition does not require Atg36. To test this more directly, we generated an *ATG36* deficient strain that is also blocked in DRP-dependent peroxisome fission (*vps1Δ/dnm1Δ/atg36Δ*) and reintroduced either Vps1 or Dnm1. Expression of either Vps1 or Dnm1 increased peroxisome number in this strain, indicating that Vps1 and Dnm1 are able to divide peroxisomes independent of ATG36 (Fig. 5B,C). Moreover, localisation of Vps1-K42A to peroxisomes in proliferating *vps1Δ/dnm1Δ/atg36Δ* cells is not affected (Fig. 5E).

Pex27 is not required for efficient pexophagy

Recruitment of Vps1 to the pexophagophore via the Atg11 and Atg36 complex was previously visualised by bimolecular fluorescence complementation (Mao et al., 2014). Indeed, in cells co-expressing Vps1-Vc and Vn-Atg11, a clear Venus signal was observed in the proximity of peroxisomes (Fig. 6A). Although a signal was observed in *atg36Δ* cells, this signal did not localise to peroxisomes. Using this

assay, we found that Vps1 recruitment to the pexophagophore is unaffected by deletion of *PEX27* (Fig. 6A). To test the efficiency of pexophagy in *pex27Δ* cells, we analysed cells expressing Pex11-GFP using fluorescence microscopy (Fig. 6B) and the accumulation of a Pex11-GFP cleavage product that forms upon entry in vacuoles as semi-quantitative measures of pexophagy (Fig. 6C) (Motley et al., 2012b). This analysis revealed that in contrast to *vps1Δ* cells, *pex27Δ* cells are unaffected in timing of the initiation and the level of pexophagy. We conclude that Pex27 is not required for pexophagy.

DISCUSSION

The dynamin-related protein Vps1 requires auxiliary factors for its recruitment and activity during a variety of membrane remodelling processes. Here we report that Vps1-dependent peroxisome fission, but not Dnm1-dependent peroxisome fission requires the peroxisomal membrane protein Pex27 and that Pex27 localises to constricted areas of peroxisomes when fission is blocked. In addition, we show that Pex27 and Vps1 are able to physically interact *in vivo* and that an increase in the level of Pex27, increases peroxisome number dependent upon Vps1. A GTPase mutant of Vps1, Vps1-K42A, that mainly localises to endosomes (Sundborger et al., 2014; Tornabene et al., 2020; Varlakhanova et al., 2018) also associates with peroxisomes and this association depends on Pex27. These observations support a model whereby Pex27 acts as a specific Vps1 cofactor on the peroxisomal membrane (Fig.7). Interestingly, Pex27 is not required during Vps1-dependent fission of peroxisomes during pexophagy.

Peroxisome multiplication is a multistep process during which peroxisomes generate a membrane protrusion that subsequently elongates and starts importing matrix proteins. Subsequently, dynamin-related proteins divide the peroxisomes at constricted areas between the bulbous parts; for review see (Schrader et al., 2016). In mammals and the yeast *H. polymorpha*, the tubulation of the peroxisomal membrane is induced by Pex11β/*Hp*Pex11. Membrane remodelling by Pex11 is coupled to recruitment of fission factors (Fis1, Drp1/Dnm1 and in mammals MFF) to sites of membrane constriction (Imoto et al., 2020; Williams et al., 2015). Pex11β/*Hp*Pex11 also acts at the scission stage as Pex11β/*Hp*Pex11 interacts

directly with Drp1 and stimulates its GTPase activity *in vitro*. Mutants that block this interaction block *in vitro* GTPase activation and peroxisome fission *in vivo* (Williams et al., 2015).

In *S. cerevisiae*, Dnm1 and Pex11 play a minor role in peroxisome multiplication that is most obvious under conditions of peroxisome proliferation (Erdmann and Blobel, 1995; Kuravi et al., 2006; Motley et al., 2008) (see also Fig. S1). On the other hand, Vps1, Pex25 and Pex27 deficient cells, display a strong reduction of peroxisome number, especially in rapidly dividing cells. Pex25 plays a crucial role in the generation of the initial protrusion and elongation of peroxisomal membrane tubules (Huber et al., 2012) and therefore resembles Pex11β in that. Elongated tubular peroxisomes characteristic of *vps1Δ/dnm1Δ* cells are indeed mostly absent in *vps1Δ/dnm1Δ/pex25Δ* cells (Fig. 2D and S1,S3I). Detailed mechanistic studies of Pex25 have not been reported but like Pex11β, Pex25 contains a predicted amphipathic helix in its N-terminal half that may be required for membrane tubulation. The role of Pex25 in elongation is also unknown but it is tempting to speculate that like *S. cerevisiae* Pex11, Pex25 is part of a membrane contact site and that the Pex25 membrane contact site allows membrane lipid flux into growing peroxisomal membrane tubules analogous to the role of the ER-Peroxisome tether ACBD4/5 and VAPB (Costello et al., 2017a; Costello et al., 2017b; Hua et al., 2017). Pex25 is required for both Vps1-dependent and Dnm1-dependent peroxisome fission. Even overexpression of these Drps cannot induce peroxisomes to divide in the absence of Pex25. The Pex25 paralogue, Pex27 is not required for elongation of peroxisomes (Fig 1A), their tubulation or their constriction (see for instance Fig 3C, 4G, 4H and S1).. Since Pex27 overexpression does not restore peroxisome number in *pex25Δ* cells, the two paralogues have evolved into proteins each with their specific function(s). We identified Pex27 as a factor specifically required for Vps1-dependent peroxisome fission. It concentrates in constricted areas of the peroxisomal membrane in cells where fission is blocked. This observation is further corroborated when Pex27-GFP is overexpressed. Pex27 concentrates on the tubules connecting the bulbous parts (Fig. 4F). These tubules however are very dimly labelled with peroxisomal matrix proteins suggesting that they are extended constrictions. Whereas Pex25 acts at early stages of peroxisome multiplication, in the protrusion and elongation stages, our data support a role for Pex27 in Vps1-

dependent fission after constriction of the peroxisomal membrane. Its position at constriction sites places Pex27 ideally to either recruit Vps1 directly or to modify the constriction site, through for instance remodelling of the membrane or recruitment of other factors, to allow local assembly of Vps1 oligomers. These options are in line with our observation that the Vps1 K42A mutant accumulates on peroxisomes dependent on Pex27. Vps1 K42A is a GTP hydrolysis mutant that forms helical assemblies in a hyper constricted state that fail to disassemble and therefore accumulate on target membranes (Tornabene et al., 2020; Varlakhanova et al., 2018). As we could not detect Vps1 K42A-GFP on peroxisomes in *vps1Δ/dnm1Δ/pex27Δ* cells, we conclude that Pex27 acts prior to Vps1 reaching its hyper constricted state on the peroxisomal membrane. We cannot exclude additional later roles for Pex27 in Vps1-dependent fission, for instance in the regulation of Vps1 GTPase activity analogous to *H. polymorpha* Pex11 and human Pex11β in the regulation of Dnm1/Drp1 (Williams et al., 2015).

On the other hand, previous overexpression studies with *PEX27* were interpreted to counteract the Pex25 function in peroxisome multiplication (Huber et al., 2012). This conclusion was based on the observation that Pex27 overexpression resulted in a partial mislocalisation of a peroxisomal matrix marker to the cytosol and decreased growth on oleate medium. We confirmed that Pex27 overexpression induces a partial block in matrix protein import (Fig. S3A). However, when using peroxisomal membrane markers, we found that Pex27 overexpression induces extensive Vps1-dependent peroxisome fission and we therefore conclude that Pex27 does not counteract Pex25 in peroxisome fission. Why Pex27 overexpression induces mislocalisation of matrix proteins is not clear but it is unrelated to the extensive fission of peroxisomes as even in cells lacking Vps1, matrix proteins were mislocalised (Fig. S3A).

Vps1 has been reported to divide larger peroxisomes to accommodate their engulfment by autophagosomal membranes and promote efficient pexophagy. Vps1 is recruited to pexophagophores via the Atg36/Atg11 pexophagy receptor complex (Mao et al., 2014). We found that neither Atg36 nor Atg11 is required for peroxisome multiplication during exponential growth and for the association of Vps1-K42A with peroxisomes. Neither did we find a requirement for Pex27 in recruitment of Vps1 to the pexophagophore nor for pexophagy.

Our results expand the set of factors that allow Vps1 to act in various membrane remodelling processes and we conclude that Vps1 function in peroxisome maintenance under different growth conditions is aided by process specific auxiliary factors.

MATERIALS AND METHODS

Strains and plasmids

Yeast strains used in this study are shown in Table S1. Yeast strains were derivatives of either BY4741 (*MATA his3Δ1 leu2Δ0 met15Δ0 ura3Δ0*) or BY4742 (*MATα his3Δ1 leu2Δ0 lys2Δ0 ura3Δ0*) obtained from the EUROSCARF consortium. Double or triple gene deletions were made by replacing the entire coding sequence of the desired gene with either *Schizosaccharomyces pombe HIS5* or *Klebsiella pneumoniae* hygromycin B phosphotransferase that confers resistance to hygromycin B (Goldstein and McCusker, 1999). pFA6a-yomNeonGreen (mNG)-spHIS5 plasmid was used as template for PCR to tag *PEX11*, and *PEX27* open reading frames at C-terminal in genome with mNG (Shaner et al., 2013).

Plasmids used in this study are listed in Table S2. *URA3* and *LEU2* centromeric plasmids were derived from Ycplac33 and Ycplac111 (Gietz and Sugino, 1988) and contained the *PGK1* terminator. These ARS1/CEN4 plasmids are present at 1-2 copies per cell (see for instance Falcon and Aris, 2000). The plasmid constructs were generated either by gap repair mechanism in yeast (Orr-Weaver and Szostak, 1983) or by conventional restriction digestion-ligation based methods in *E. coli* (Cohen et al., 1973). Constitutive expression of HcRed-PTS1, mNG-PTS1, mKate2-PTS1 and GFP was under either *HIS3* or *Tpi1* promoter and the conditional expression plasmids contained the *GAL1* promoter. *DNM1* and *VPS1* overexpression was achieved using *TPI1* promoter and were described previously (Motley et al., 2008). Expression of Vps1-GFP and Vps1-K42A-GFP was achieved through the Vps1 promoter and Pex27-ProtA was under control of its own promoter. Plasmids and strains are available upon request.

Growth conditions

For the screen presented in Fig S1, cells were grown overnight in a defined selective 2% glucose medium at 30ºC. For analysis of phenotypes by microscopy, cells were subsequently diluted to OD_{600}=0.1 in a fresh selective 2% glucose medium and grown for at least three cell divisions (6 h), prior to imaging. Certain phenotypes are sensitive to cell growth rate. For instance, peroxisome inheritance defects are compensated for by de novo formation and the number of cells without peroxisomes increases in exponential growing cultures vs stationary phase cultures (Hettema and

Motley, 2009). Likewise, peroxisome number in pexophagy mutants is affected by growth rate (Nuttall et al., 2014). Therefore, in subsequent experiments, we made sure that overnight culture did not reach the stationary phase before they were diluted to OD_{600}=0.1 in the morning. Where the induction of a reporter protein was required, cells were transferred to selective galactose medium at OD_{600}=0.1 and grown for the time indicated in the figures and text. Yeast cells were grown at 30°C in either of the following mediums: rich YPD media (1% yeast extract, 2% peptone, 2% glucose), minimal media 2 (YM2) for the selection of the uracil prototrophic marker (carbon source, 0.17% yeast nitrogen base without amino acids and ammonium sulphate, 0.5% ammonium sulphate, 1% casamino acids) or minimal media 1 (YM1) for the selection of all prototrophic markers (carbon source, 0.17% yeast nitrogen base without amino acids and ammonium sulphate, 0.5% ammonium sulphate). Regarding the carbon sources, glucose and galactose were added to 2% (w/v). For induction of peroxisome proliferation, cells were transferred to oleate medium (YM2 oleate: YM2 plus 0.12% oleate (v/v), 0.2% Tween-40s (v/v), 0.1% yeast extract) at a 1/10 overnight dilution. Pexophagy was induced by transferring cells to starvation medium lacking a nitrogen source (SD-N; 0.17% yeast nitrogen base without amino acids and ammonium sulphate, 2% glucose) (Hutchins et al., 1999; Lynch-Day and Klionsky, 2010). The appropriate amino acid stocks were added to minimal media as required. In all, 10 OD_{600} units were collected at selected time points as indicated in the figures and text. Cells were either analysed by immunoblotting or by fluorescence microscopy. For peroxisome quantification the budding cells were considered as single cells. Mating experiments were performed as described previously (Motley and Hettema, 2007). Briefly, for mating, 1 OD_{600} unit of cells of MATα cells were first induced with galactose for 3 h and subsequently chased for 2 h on YPD before they were mixed with 1 OD_{600} unit of MAT A cells, pelleted, and spotted onto a prewarmed YPD plate and incubated at 30°C for 2 h before imaging. The vacuolar membrane was stained with FM4-64 as previously described (Vida and Emr, 1995).

Image acquisition

Cells were analysed with a microscope (Axiovert 200M; Carl Zeiss) equipped with an Exfo X-cite 120 excitation light source, band pass filters (Carl Zeiss and Chroma Technology Corp.), an α Plan-Fluar 100 x 1.45 NA and Plan-Apochromat 63 x 1.4 NA objective lens (Carl Zeiss) and a digital camera (Orca ER; Hamamatsu Photonics). Image acquisition was performed using Volocity software (PerkinElmer). Fluorescence images were collected as 0.25/0.5 µm Z stacks, merged into one plane in Openlab (PerkinElmer), and processed further in Photoshop (Adobe). Brightfield images were collected in one plane and processed where necessary to highlight circumference of the cells. Each imaging experiment was performed at least 3 times, and representative images are shown. For quantitation, a single experiment was used. For localization of Pex11-mNG and Pex27-mNG *in vivo*, cells were imaged

with DeltaVision/GE OMX optical microscope equipped with laser lines (488 nm and 568 nm) and 60 x 1.42 NA oil Plan-Apochromat to perform structured illumination microscopy (SIM). Image acquisition was performed using DeltaVision OMX SoftWoRx 6.0 software. Fluorescence images were collected as 0.25 µm Z stacks, merged into one plane in Fiji (Schindelin et al., 2012), and processed further in Adobe Photoshop. To immobilise cells, a 2% agarose gel pad containing minimal growth medium was prepared into a glass bottom 35mm µ-dish (Ibidi). The cells were grown logarithmically and 20 µl culture was supplied under the gel pad and spread uniformly by gently pressing the gel pad from the top.

Immunoblotting

For preparation of extracts by alkaline lysis, cells were centrifuged, and pellets resuspended in 0.2M NaOH and 0.2% β-mercaptoethanol and left on ice for 10 min. Soluble protein was precipitated by addition of 5% TCA and incubation on ice for further 15 min. Following centrifugation (13 000 g, 5 min, 4°C), the pellet was resuspended in 10 µl 1M Tris–HCl (pH 9.4) and 90 µl 1x SDS–PAGE sample loading buffer and boiled for 10 min at 95°C. Samples (0.25–1 OD_{600} equivalent) were resolved by SDS–PAGE followed by immunoblotting. Blots were blocked in 2% (w/v) fat-free Marvel milk in TBS-Tween-20 (50mM Tris–HCl pH 7.6, 150mM NaCl, 0.1% (v/v) Tween-20). GFP-tagged proteins were detected using monoclonal anti-GFP (mouse IgG monoclonal antibody clone 7.1 and 13.1; 1:3000; Roche, 11814460001). Pex27-ProtA and Pex27-TAP were detected by peroxidase-anti-peroxidase (PAP) (rabbit; 1:4000; Sigma, P1291). Vps1 was detected with polyclonal anti-Vps1 (rat; 1:10000; gift of Kathryn Ayscough). Specificity of this antiserum is shown by lack of signal in *vps1Δ* cells in figure 1C. Secondary antibody was HRP-linked anti-mouse polyclonal (goat; 1:4000; Bio-Rad) or HRP-linked anti-rat polyclonal (rabbit; 1:10000, Sigma, A5795). Detection was achieved using enhanced chemiluminescence reagents (GE healthcare) and chemiluminescence imaging.

Coimmunoprecipitation

For immunoprecipitation experiments we transformed Pex27-TAP-tagged cells (Ghaemmaghami et al., 2003) with a centromeric plasmid encoding GFP-PTS1 under control of the TPI1 promoter (pEH012) or Vps1-GFP under control of its endogenous promoter (pKA1078, Ayscough lab) or empty plasmid (Ycplac33). Logarithmically growing 50-60OD_{600} cells were harvested and washed once with 50mM HEPES-KOH pH7.6 before freezing at -80°C. The cell pellet was thawed and resuspended in 600 µl of cold lysis buffer (50mM HEPES-KOH, pH 7.6, 150mM KCl, 100mM β-glycerol phosphate, 25mM NaF, 1mM EGTA, 1mM $MgCl_2$, 0.15% Tween-20, Protease inhibitor cocktail). Subsequently, 400 µl of acid washed glass beads were added to the above mixture. The cells were lysed by means of glass bead beater for 2X 30 sec rounds at top speed and 2 min on ice after each round. The

tubes were centrifuged for 5 min at 13000rpm, 4°C. Approximately 400 µl supernatant was collected and replaced with 400 µl of lysis buffer and the tubes were beaten and followed by centrifugation again as mentioned above. The supernatants were pooled together and further cleared by centrifugation (5 min at 13000rpm, 4°C). The clear supernatant was transferred to the affinity purification beads pre-equilibrated in the lysis buffer. From cell lysate samples 45 µl was taken before treatment with affinity beads as input material. The tubes were incubated on a rotating wheel at 4°C for 2 h and then washed three times with the lysis buffer supplemented with 10% glycerol and no protease inhibitors. Then the beads were transferred to the fresh tube and washed once more before adding 100 µl 1x protein loading dye. The samples were boiled at 95°C for 10 min and analysed by western blot. GFP fusions were detected using anti-GFP, endogenous Vps1 was detected with anti-Vps1 and Pex27-TAP was detected with PAP. For further detail see materials and methods section Immunoblotting.

ACKNOWLEDGEMENTS

REFERENCES

Antonny, B., C. Burd, P. De Camilli, E. Chen, O. Daumke, K. Faelber, M. Ford, V.A. Frolov, A. Frost, J.E. Hinshaw, T. Kirchhausen, M.M. Kozlov, M. Lenz, H.H. Low, H. McMahon, C. Merrifield, T.D. Pollard, P.J. Robinson, A. Roux, and S. Schmid. 2016. Membrane fission by dynamin: what we know and what we need to know. *EMBO J.* 35:2270-2284.

Bonekamp, N.A., S. Grille, M.J. Cardoso, M. Almeida, M. Aroso, S. Gomes, A.C. Magalhaes, D. Ribeiro, M. Islinger, and M. Schrader. 2013. Self-interaction of human Pex11pbeta during peroxisomal growth and division. *PLoS One.* 8:e53424.

Byrne, K.P., and K.H. Wolfe. 2005. The Yeast Gene Order Browser: combining curated homology and syntenic context reveals gene fate in polyploid species. *Genome Res.* 15:1456-1461.

Carmichael, R.E., and M. Schrader. 2022. Determinants of Peroxisome Membrane Dynamics. *Front Physiol.* 13:834411.

Chang, J., M.J. Klute, R.J. Tower, F.D. Mast, J.B. Dacks, and R.A. Rachubinski. 2015. An ancestral role in peroxisome assembly is retained by the divisional peroxin Pex11 in the yeast Yarrowia lipolytica. *J Cell Sci.* 128:1327-1340.

Chi, R.J., J. Liu, M. West, J. Wang, G. Odorizzi, and C.G. Burd. 2014. Fission of SNX-BAR-coated endosomal retrograde transport carriers is promoted by the dynamin-related protein Vps1. *J Cell Biol*. 204:793-806.

Cohen, S.N., A.C. Chang, H.W. Boyer, and R.B. Helling. 1973. Construction of biologically functional bacterial plasmids in vitro. *Proc Natl Acad Sci U S A*. 70:3240-3244.

Costello, J.L., I.G. Castro, C. Hacker, T.A. Schrader, J. Metz, D. Zeuschner, A.S. Azadi, L.F. Godinho, V. Costina, P. Findeisen, A. Manner, M. Islinger, and M. Schrader. 2017a. ACBD5 and VAPB mediate membrane associations between peroxisomes and the ER. *J Cell Biol*. 216:331-342.

Costello, J.L., I.G. Castro, T.A. Schrader, M. Islinger, and M. Schrader. 2017b. Peroxisomal ACBD4 interacts with VAPB and promotes ER-peroxisome associations. *Cell Cycle*. 16:1039-1045.

Ebberink, M.S., J. Koster, G. Visser, F. Spronsen, I. Stolte-Dijkstra, G.P. Smit, J.M. Fock, S. Kemp, R.J. Wanders, and H.R. Waterham. 2012. A novel defect of peroxisome division due to a homozygous non-sense mutation in the PEX11beta gene. *J Med Genet*. 49:307-313.

Erdmann, R., and G. Blobel. 1995. Giant peroxisomes in oleic acid-induced Saccharomyces cerevisiae lacking the peroxisomal membrane protein Pmp27p. *J Cell Biol*. 128:509-523.

Esposito, M., S. Hermann-Le Denmat, and A. Delahodde. 2019. Contribution of ERMES subunits to mature peroxisome abundance. *PLoS One*. 14:e0214287.

Ferguson, S.M., and P. De Camilli. 2012. Dynamin, a membrane-remodelling GTPase. *Nat Rev Mol Cell Biol*. 13:75-88.

Ghaemmaghami, S., W.K. Huh, K. Bower, R.W. Howson, A. Belle, N. Dephoure, E.K. O'Shea, and J.S. Weissman. 2003. Global analysis of protein expression in yeast. *Nature*. 425:737-741.

Gietz, R.D., and A. Sugino. 1988. New yeast-Escherichia coli shuttle vectors constructed with in vitro mutagenized yeast genes lacking six-base pair restriction sites. *Gene*. 74:527-534.

Goldstein, A.L., and J.H. McCusker. 1999. Three new dominant drug resistance cassettes for gene disruption in Saccharomyces cerevisiae. *Yeast*. 15:1541-1553.

Hettema, E.H., W. Girzalsky, M. van Den Berg, R. Erdmann, and B. Distel. 2000. Saccharomyces cerevisiae pex3p and pex19p are required for proper localization and stability of peroxisomal membrane proteins. *EMBO J*. 19:223-233.

Hettema, E.H., and A.M. Motley. 2009. How peroxisomes multiply. *J Cell Sci*. 122:2331-2336.

Hoepfner, D., M. van den Berg, P. Philippsen, H.F. Tabak, and E.H. Hettema. 2001. A role for Vps1p, actin, and the Myo2p motor in peroxisome abundance and inheritance in Saccharomyces cerevisiae. *J Cell Biol*. 155:979-990.

Honsho, M., S. Yamashita, and Y. Fujiki. 2016. Peroxisome homeostasis: Mechanisms of division and selective degradation of peroxisomes in mammals. *Biochim Biophys Acta*. 1863:984-991.

Hua, R., D. Cheng, E. Coyaud, S. Freeman, E. Di Pietro, Y. Wang, A. Vissa, C.M. Yip, G.D. Fairn, N. Braverman, J.H. Brumell, W.S. Trimble, B. Raught, and P.K. Kim. 2017. VAPs and ACBD5 tether peroxisomes to the ER for peroxisome maintenance and lipid homeostasis. *J Cell Biol*. 216:367-377.

Huber, A., J. Koch, F. Kragler, C. Brocard, and A. Hartig. 2012. A subtle interplay between three Pex11 proteins shapes de novo formation and fission of peroxisomes. *Traffic*. 13:157-167.

Hutchins, M.U., M. Veenhuis, and D.J. Klionsky. 1999. Peroxisome degradation in Saccharomyces cerevisiae is dependent on machinery of macroautophagy and the Cvt pathway. *J Cell Sci*. 112 (Pt 22):4079-4087.

Imoto, Y., K. Itoh, and Y. Fujiki. 2020. Molecular Basis of Mitochondrial and Peroxisomal Division Machineries. *Int J Mol Sci*. 21.

Itoyama, A., M. Honsho, Y. Abe, A. Moser, Y. Yoshida, and Y. Fujiki. 2012. Docosahexaenoic acid mediates peroxisomal elongation, a prerequisite for peroxisome division. *J Cell Sci*. 125:589-602.

Jansen, R.L.M., C. Santana-Molina, M. van den Noort, D.P. Devos, and I.J. van der Klei. 2021. Comparative Genomics of Peroxisome Biogenesis Proteins: Making Sense of the PEX Proteins. *Front Cell Dev Biol*. 9:654163.

Jimah, J.R., and J.E. Hinshaw. 2019. Structural Insights into the Mechanism of Dynamin Superfamily Proteins. *Trends Cell Biol*. 29:257-273.

Kuravi, K., S. Nagotu, A.M. Krikken, K. Sjollema, M. Deckers, R. Erdmann, M. Veenhuis, and I.J. van der Klei. 2006. Dynamin-related proteins Vps1p and Dnm1p control peroxisome abundance in Saccharomyces cerevisiae. *J Cell Sci*. 119:3994-4001.

Lewis, M.J., B.J. Nichols, C. Prescianotto-Baschong, H. Riezman, and H.R. Pelham. 2000. Specific retrieval of the exocytic SNARE Snc1p from early yeast endosomes. *Mol Biol Cell*. 11:23-38.

Liu, X., X. Wen, and D.J. Klionsky. 2018. ER-mitochondria contacts are required for pexophagy in Saccharomyces cerevisiae. *Contact (Thousand Oaks)*. 2.

Lukehart, J., C. Highfill, and K. Kim. 2013. Vps1, a recycling factor for the traffic from early endosome to the late Golgi. *Biochem Cell Biol*. 91:455-465.

Lynch-Day, M.A., and D.J. Klionsky. 2010. The Cvt pathway as a model for selective autophagy. *FEBS Lett*. 584:1359-1366.

Ma, M., C.G. Burd, and R.J. Chi. 2017. Distinct complexes of yeast Snx4 family SNX-BARs mediate retrograde trafficking of Snc1 and Atg27. *Traffic*. 18:134-144.

Mao, K., X. Liu, Y. Feng, and D.J. Klionsky. 2014. The progression of peroxisomal degradation through autophagy requires peroxisomal division. *Autophagy*. 10:652-661.

Marshall, P.A., Y.I. Krimkevich, R.H. Lark, J.M. Dyer, M. Veenhuis, and J.M. Goodman. 1995. Pmp27 promotes peroxisomal proliferation. *J Cell Biol*. 129:345-355.

Mattiazzi Usaj, M., M. Brloznik, P. Kaferle, M. Zitnik, H. Wolinski, F. Leitner, S.D. Kohlwein, B. Zupan, and U. Petrovic. 2015. Genome-Wide Localization Study of Yeast Pex11 Identifies Peroxisome-Mitochondria Interactions through the ERMES Complex. *J Mol Biol*. 427:2072-2087.

Mindthoff, S., S. Grunau, L.L. Steinfort, W. Girzalsky, J.K. Hiltunen, R. Erdmann, and V.D. Antonenkov. 2016. Peroxisomal Pex11 is a pore-forming protein homologous to TRPM channels. *Biochim Biophys Acta*. 1863:271-283.

Motley, A.M., P.C. Galvin, L. Ekal, J.M. Nuttall, and E.H. Hettema. 2015. Reevaluation of the role of Pex1 and dynamin-related proteins in peroxisome membrane biogenesis. *J Cell Biol*. 211:1041-1056.

Motley, A.M., and E.H. Hettema. 2007. Yeast peroxisomes multiply by growth and division. *J Cell Biol*. 178:399-410.

Motley, A.M., J.M. Nuttall, and E.H. Hettema. 2012a. Atg36: the Saccharomyces cerevisiae receptor for pexophagy. *Autophagy*. 8:1680-1681.

Motley, A.M., J.M. Nuttall, and E.H. Hettema. 2012b. Pex3-anchored Atg36 tags peroxisomes for degradation in Saccharomyces cerevisiae. *EMBO J*. 31:2852-2868.

Motley, A.M., G.P. Ward, and E.H. Hettema. 2008. Dnm1p-dependent peroxisome fission requires Caf4p, Mdv1p and Fis1p. *J Cell Sci*. 121:1633-1640.

Nagotu, S., A.M. Krikken, M. Otzen, J.A. Kiel, M. Veenhuis, and I.J. van der Klei. 2008. Peroxisome fission in Hansenula polymorpha requires Mdv1 and Fis1, two proteins also involved in mitochondrial fission. *Traffic*. 9:1471-1484.

Nothwehr, S.F., E. Conibear, and T.H. Stevens. 1995. Golgi and vacuolar membrane proteins reach the vacuole in vps1 mutant yeast cells via the plasma membrane. *J Cell Biol*. 129:35-46.

Nuttall, J.M., A.M. Motley, and E.H. Hettema. 2014. Deficiency of the exportomer components Pex1, Pex6, and Pex15 causes enhanced pexophagy in Saccharomyces cerevisiae. *Autophagy*. 10:835-845.

Opalinski, L., J.A. Kiel, C. Williams, M. Veenhuis, and I.J. van der Klei. 2011. Membrane curvature during peroxisome fission requires Pex11. *EMBO J*. 30:5-16.

Orr-Weaver, T.L., and J.W. Szostak. 1983. Yeast recombination: the association between double-strand gap repair and crossing-over. *Proc Natl Acad Sci U S A*. 80:4417-4421.

Peters, C., T.L. Baars, S. Buhler, and A. Mayer. 2004. Mutual control of membrane fission and fusion proteins. *Cell*. 119:667-678.

Praefcke, G.J., and H.T. McMahon. 2004. The dynamin superfamily: universal membrane tubulation and fission molecules? *Nat Rev Mol Cell Biol*. 5:133-147.

Ross, J.A., Y. Chen, J. Muller, B. Barylko, L. Wang, H.B. Banks, J.P. Albanesi, and D.M. Jameson. 2011. Dimeric endophilin A2 stimulates assembly and GTPase activity of dynamin 2. *Biophys J*. 100:729-737.

Rottensteiner, H., K. Stein, E. Sonnenhol, and R. Erdmann. 2003. Conserved function of pex11p and the novel pex25p and pex27p in peroxisome biogenesis. *Mol Biol Cell*. 14:4316-4328.

Roux, A., G. Koster, M. Lenz, B. Sorre, J.B. Manneville, P. Nassoy, and P. Bassereau. 2010. Membrane curvature controls dynamin polymerization. *Proc Natl Acad Sci U S A*. 107:4141-4146.

Schindelin, J., I. Arganda-Carreras, E. Frise, V. Kaynig, M. Longair, T. Pietzsch, S. Preibisch, C. Rueden, S. Saalfeld, B. Schmid, J.Y. Tinevez, D.J. White, V. Hartenstein, K. Eliceiri, P. Tomancak, and A. Cardona. 2012. Fiji: an open-source platform for biological-image analysis. *Nat Methods*. 9:676-682.

Schrader, M., J.L. Costello, L.F. Godinho, A.S. Azadi, and M. Islinger. 2016. Proliferation and fission of peroxisomes - An update. *Biochim Biophys Acta*. 1863:971-983.

Schrader, T.A., R.E. Carmichael, M. Islinger, J.L. Costello, C. Hacker, N.A. Bonekamp, J.H. Weishaupt, P.M. Andersen, and M. Schrader. 2022. PEX11beta and FIS1 cooperate in peroxisome division independently of mitochondrial fission factor. *J Cell Sci*. 135.

Shaner, N.C., G.G. Lambert, A. Chammas, Y. Ni, P.J. Cranfill, M.A. Baird, B.R. Sell, J.R. Allen, R.N. Day, M. Israelsson, M.W. Davidson, and J. Wang. 2013. A bright monomeric green fluorescent protein derived from Branchiostoma lanceolatum. *Nat Methods*. 10:407-409.

Smaczynska-de, R., II, E.G. Allwood, S. Aghamohammadzadeh, E.H. Hettema, M.W. Goldberg, and K.R. Ayscough. 2010. A role for the dynamin-like protein Vps1 during endocytosis in yeast. *J Cell Sci*. 123:3496-3506.

Smaczynska-de, R., II, E.G. Allwood, R. Mishra, W.I. Booth, S. Aghamohammadzadeh, M.W. Goldberg, and K.R. Ayscough. 2012. Yeast dynamin Vps1 and amphiphysin Rvs167 function together during endocytosis. *Traffic*. 13:317-328.

Smaczynska-de, R., II, C.J. Marklew, S.E. Palmer, E.G. Allwood, and K.R. Ayscough. 2019. Mutation of key lysine residues in the Insert B region of the yeast dynamin Vps1 disrupts lipid binding and causes defects in endocytosis. *PLoS One*. 14:e0215102.

Smith, J.J., M. Marelli, R.H. Christmas, F.J. Vizeacoumar, D.J. Dilworth, T. Ideker, T. Galitski, K. Dimitrov, R.A. Rachubinski, and J.D. Aitchison. 2002. Transcriptome profiling to identify genes involved in peroxisome assembly and function. *J Cell Biol*. 158:259-271.

Su, J., A.S. Thomas, T. Grabietz, C. Landgraf, R. Volkmer, S.J. Marrink, C. Williams, and M.N. Melo. 2018. The N-terminal amphipathic helix of Pex11p self-interacts to induce membrane remodelling during peroxisome fission. *Biochim Biophys Acta Biomembr*. 1860:1292-1300.

Sundborger, A.C., S. Fang, J.A. Heymann, P. Ray, J.S. Chappie, and J.E. Hinshaw. 2014. A dynamin mutant defines a superconstricted prefission state. *Cell Rep*. 8:734-742.

Suzuki, S.W., A. Oishi, N. Nikulin, J.R. Jorgensen, M.G. Baile, and S.D. Emr. 2021. A PX-BAR protein Mvp1/SNX8 and a dynamin-like GTPase Vps1 drive endosomal recycling. *Elife*. 10.

Takei, K., V.I. Slepnev, V. Haucke, and P. De Camilli. 1999. Functional partnership between amphiphysin and dynamin in clathrin-mediated endocytosis. *Nat Cell Biol*. 1:33-39.

Tam, Y.Y., J.C. Torres-Guzman, F.J. Vizeacoumar, J.J. Smith, M. Marelli, J.D. Aitchison, and R.A. Rachubinski. 2003. Pex11-related proteins in peroxisome dynamics: a role for the novel peroxin Pex27p in controlling peroxisome size and number in Saccharomyces cerevisiae. *Mol Biol Cell*. 14:4089-4102.

Tornabene, B.A., N.V. Varlakhanova, C.J. Hosford, J.S. Chappie, and M.G.J. Ford. 2020. Structural and functional characterization of the dominant negative P-loop lysine mutation in the dynamin superfamily protein Vps1. *Protein Sci*. 29:1416-1428.

Tower, R.J., A. Fagarasanu, J.D. Aitchison, and R.A. Rachubinski. 2011. The peroxin Pex34p functions with the Pex11 family of peroxisomal divisional proteins to regulate the peroxisome population in yeast. *Mol Biol Cell*. 22:1727-1738.

van Roermund, C.W., H.F. Tabak, M. van Den Berg, R.J. Wanders, and E.H. Hettema. 2000. Pex11p plays a primary role in medium-chain fatty acid oxidation, a process that affects peroxisome number and size in Saccharomyces cerevisiae. *J Cell Biol*. 150:489-498.

Varlakhanova, N.V., F.J.D. Alvarez, T.M. Brady, B.A. Tornabene, C.J. Hosford, J.S. Chappie, P. Zhang, and M.G.J. Ford. 2018. Structures of the fungal dynamin-related protein Vps1 reveal a unique, open helical architecture. *J Cell Biol*. 217:3608-3624.

Vida, T.A., and S.D. Emr. 1995. A new vital stain for visualizing vacuolar membrane dynamics and endocytosis in yeast. *J Cell Biol*. 128:779-792.

Williams, C., L. Opalinski, C. Landgraf, J. Costello, M. Schrader, A.M. Krikken, K. Knoops, A.M. Kram, R. Volkmer, and I.J. van der Klei. 2015. The membrane remodeling protein Pex11p activates the GTPase Dnm1p during peroxisomal fission. *Proc Natl Acad Sci U S A*. 112:6377-6382.

Wilsbach, K., and G.S. Payne. 1993. Vps1p, a member of the dynamin GTPase family, is necessary for Golgi membrane protein retention in Saccharomyces cerevisiae. *EMBO J*. 12:3049-3059.

Wroblewska, J.P., L.D. Cruz-Zaragoza, W. Yuan, A. Schummer, S.G. Chuartzman, R. de Boer, S. Oeljeklaus, M. Schuldiner, E. Zalckvar, B. Warscheid, R. Erdmann, and I.J. van der Klei. 2017. Saccharomyces cerevisiae cells lacking Pex3 contain membrane vesicles that harbor a subset of peroxisomal membrane proteins. *Biochim Biophys Acta Mol Cell Res*. 1864:1656-1667.

Yoshida, Y., H. Niwa, M. Honsho, A. Itoyama, and Y. Fujiki. 2015. Pex11mediates peroxisomal proliferation by promoting deformation of the lipid membrane. *Biol Open*. 4:710-721.

Figures
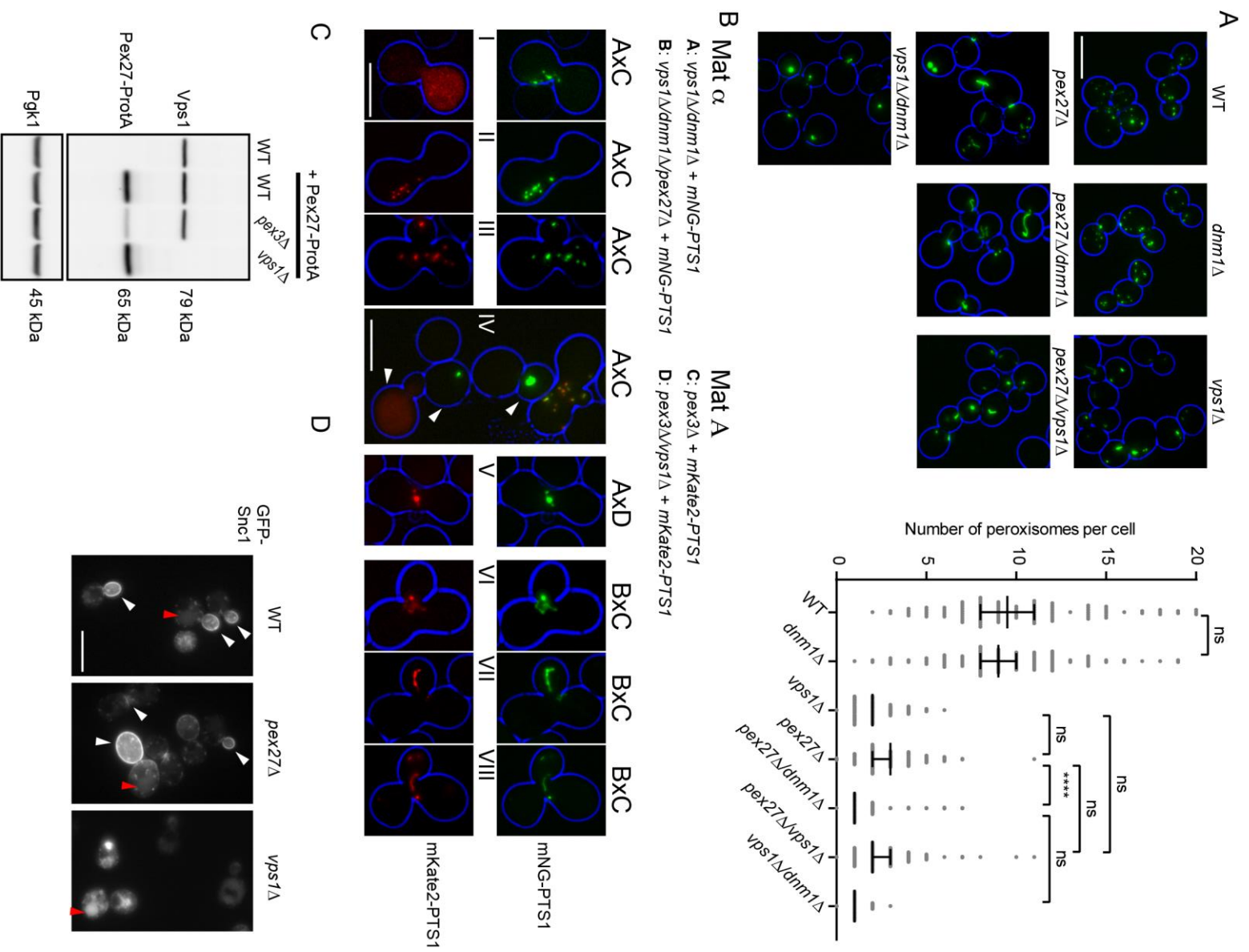
Fig. 1. Pex27 is required for Vps1-dependent peroxisome fission. (A) Epifluorescence microscopy images captured from cells expressing mNeonGreen (mNG)-PTS1 that were grown for extended periods in log phase on 2% glucose-containing medium. Representative images are shown. Peroxisome numbers were quantified for >100 budding cells for each strain grown. Bars in the graph indicate median with 95% confidence interval for mean. Statistical significance analysis was performed using Kruskal-Wallis test where, p values are for * <0.05, ** <0.01, *** <0.001, **** <0.0001, ns stands for not significant. (B) Peroxisomes in *Matα vps1Δ/dnm1Δ* + mNG-PTS1 and *vps1Δ/dnm1Δ/pex27Δ* + mNG-PTS1 cells were pulse labelled with mNG-PTS1 under control of the inducible *GAL1* promoter (pulse 3 h of galactose, chase 2h glucose) and mated with MatA *pex3Δ* and *pex3Δ/vps1Δ* cells constitutively expressing mKate2-PTS1 for 2-4 h before imaging. After cell fusion and cytoplasmic mixing, mKate2-PTS1 is imported into the mNG-labelled peroxisomal structures, which, in the presence of Vps1 and Pex27 are divided into multiple peroxisomes (I,II,III). Arrows in IV indicate cells that have not mated. No fission occurs of pre-labelled peroxisomes that lack Vps1 (V) or when the *pex3Δ* mating partner lacks Pex27 (VI,VII,VIII). Cell circumference is labelled in blue. (C) Pex27-ProtA was expressed from a centromeric plasmid under control of its own promoter. This plasmid was transformed into WT, *vps1Δ* and *pex3Δ* cells. Western blot analysis of lysates of the indicated strains using anti-Vps1 and peroxidase anti-peroxidase to detect Vps1 and Pex27-ProtA, respectively. Pgk1 was used as loading control. (D) Pex27 is not required for GFP-Snc1 recycling through the endosomal system. Representative images captured from cultures of cells expressing GFP-Snc1 that were grown in log phase on 2% glucose-containing medium. White arrows indicate GFP-Snc1 in regions of polarised growth, red arrows indicate vacuoles. (A,B,D) images are flattened *z*-stacks. Scale bar: 5 µm.
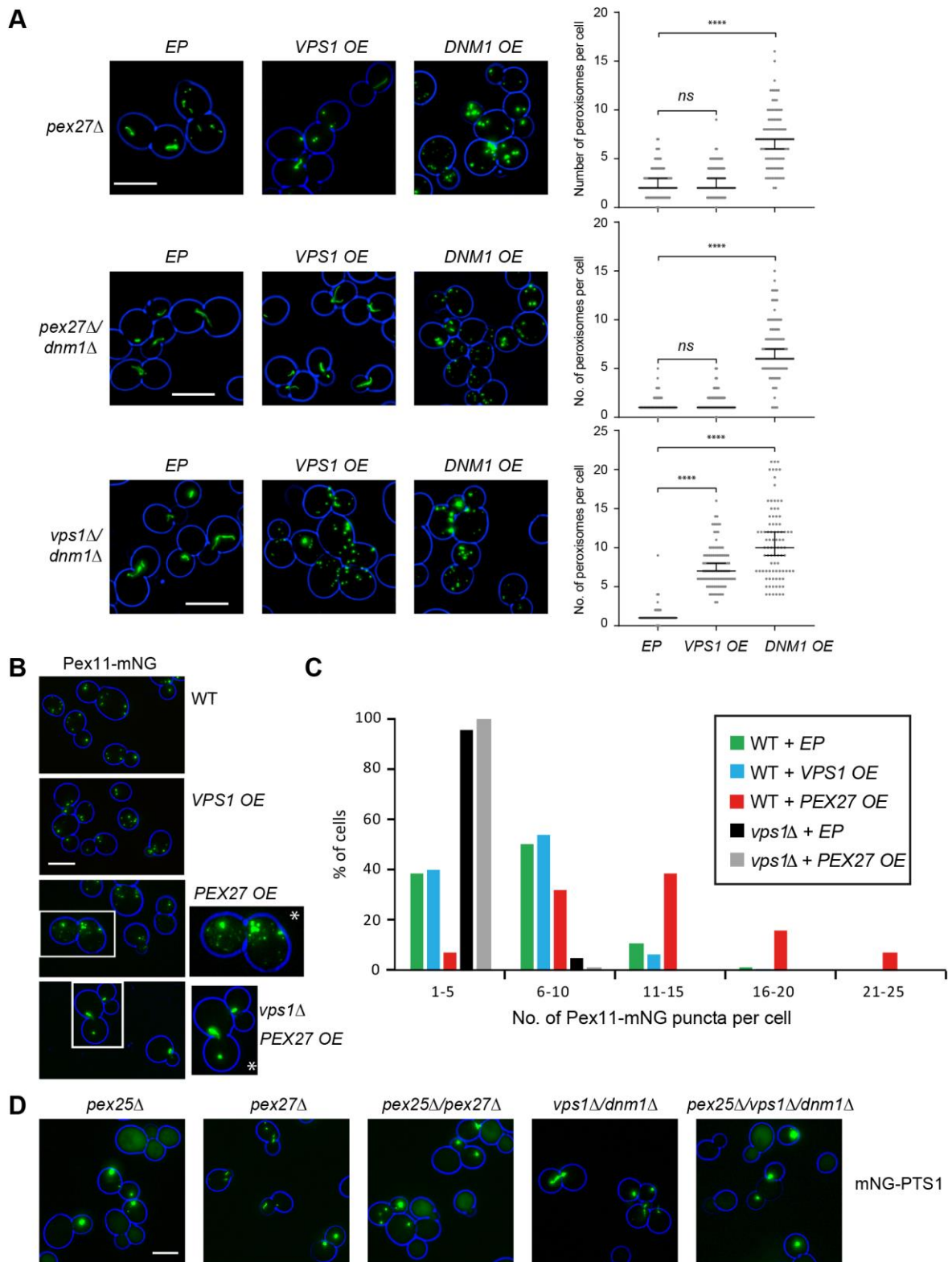
Fig. 2. Pex27 levels are limiting for Vps1-dependent peroxisome fission. (A) Vps1 overexpression does not restore peroxisome fission in either *pex27Δ* or *dnm1Δ* /*pex27Δ* cells in contrast to overexpression of Dnm1. Strains express mNG-PTS1

from a constitutive promoter. Peroxisome numbers were quantified for >100 for top and middle panel and > 89 for bottom panel budding cells for each strain grown. Bars in the graph indicate median with 95% confidence interval for mean. Statistical significance analysis was performed using Kruskal-Wallis test where, p values are for ** <0.01, ns stands for not significant. (B) Overexpression of Pex27 but not of Vps1 leads to increase in peroxisomal membrane structures dependent on the presence of Vps1. Pex11 was C-terminally tagged in the genome with mNG. * Boxed cells are further magnified and the level of green fluorescence is enhanced. (C) Quantitation of (B) where more than 100 cells were analysed for peroxisome number. (D) Epistatic analysis shows Pex25 acts upstream of Pex27 and Vps1 and Dnm1. Epifluorescence microscopy images captured from cells expressing mNG-PTS1 (A,D) or Pex11-mNG (B,C) that were grown for extended periods on 2% glucose-containing medium are representative for 3 independent imaging experiments. Images are flattened *z*-stacks. Cell circumference is labelled in blue. Scale bar: 5 µm. OE, overexpression; EP, empty plasmid control.
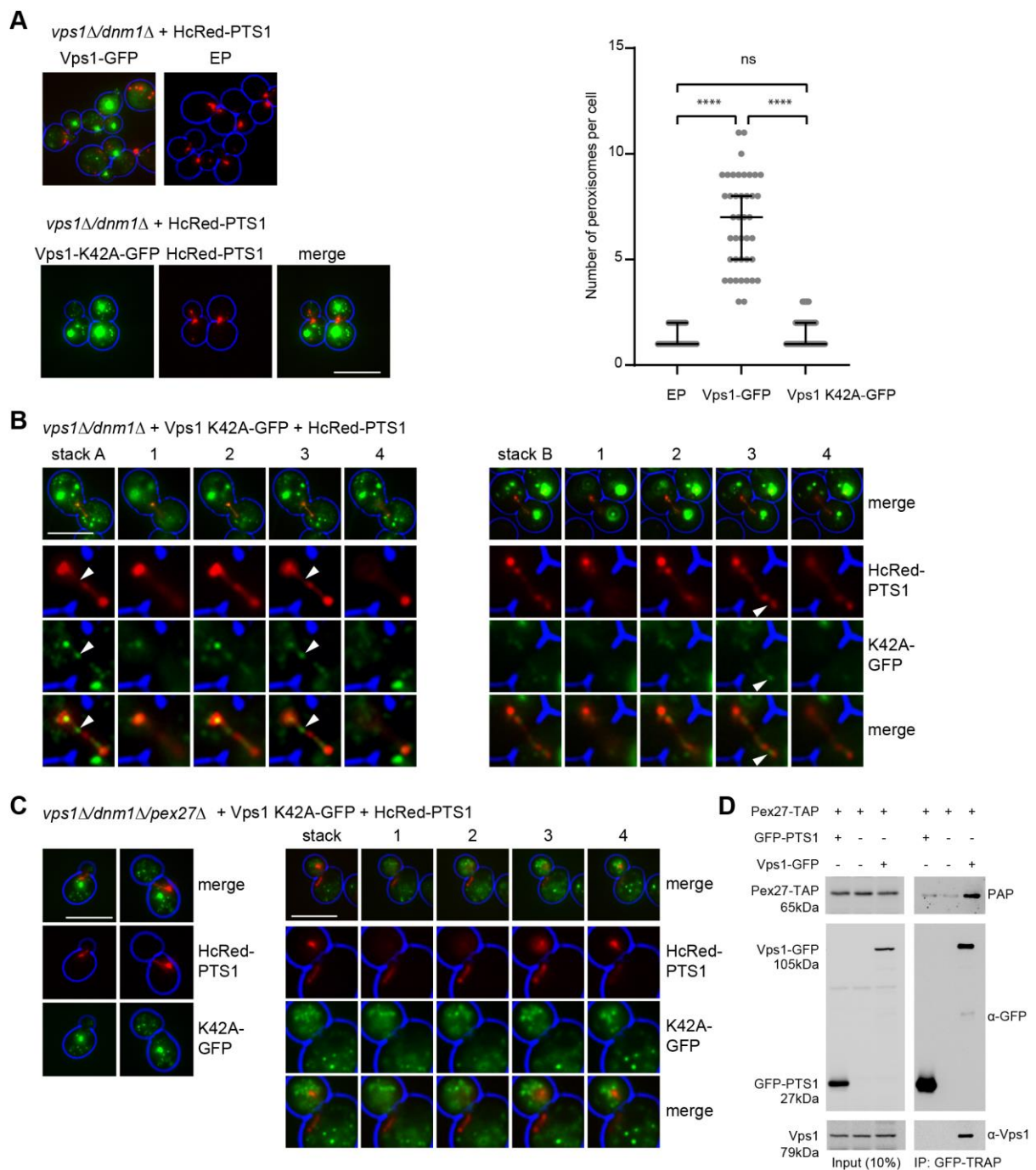
Fig. 3. Vps1 accumulation on peroxisomes requires Pex27. (A,B,C) Representative epifluorescence microscopy images of *vps1Δ/dnm1Δ* co-expressing HcRed-PTS1 and either Vps1-GFP or Vps1-K42A-GFP. (A) Vps1-GFP but not Vps1-K42A-GFP restores peroxisome fission in *vps1Δ/dnm1Δ* cells. Peroxisome numbers were quantified from >28 budding cells for each strain grown. Bars in the graph indicate median with 95% confidence interval for mean. Statistical significance analysis was performed using Kruskal-Wallis test where, p values are for ****

<0.0001. (B) Vps1-K42A-GFP associates with peroxisomes and is observed along constricted regions of the elongated peroxisome. (B) Stack A and B are separate examples of flattened *z*-stacks, numbers 1-4 indicate individual slices 0.5 µm apart. Bottom 3 rows are zoomed in. White arrows indicate examples of Vps1 K42A-GFP puncta along narrow areas of the peroxisomal tube juxtaposed to more bulbous areas of the peroxisome (C) Vps1-K42A-GFP does not enrich on peroxisomes in *vps1Δ*/*dnm1Δ*/*pex27Δ* cells. Right hand panel example of a flattened *z*-stack, numbers 1-4 indicate individual slices 0.5 µm apart. Bottom 3 rows are zoomed in. (A,B,C) Cell circumference is labelled in blue. Scale bar: 5 µm. (D) Co-immunoprecipitation analysis of Pex27-TAP tagged strain expressing either Vps1-GFP under control of its own promoter or GFP-PTS1 under control of the *TPI1* promoter from a centromeric plasmid. Vps1-GFP fusions were immunoprecipitated using GFP-nanobody beads (GFP-TRAP, Chromotek). IP samples and inputs were analysed by western blotting using antibodies against ScVps1, GFP to detect GFP fusion proteins. Pex27-TAP was detected using the peroxidase-anti-peroxidase (PAP) antibody. Pex27-TAP interacts with Vps1-GFP. Vps1-GFP also co-precipitates endogenous Vps1.
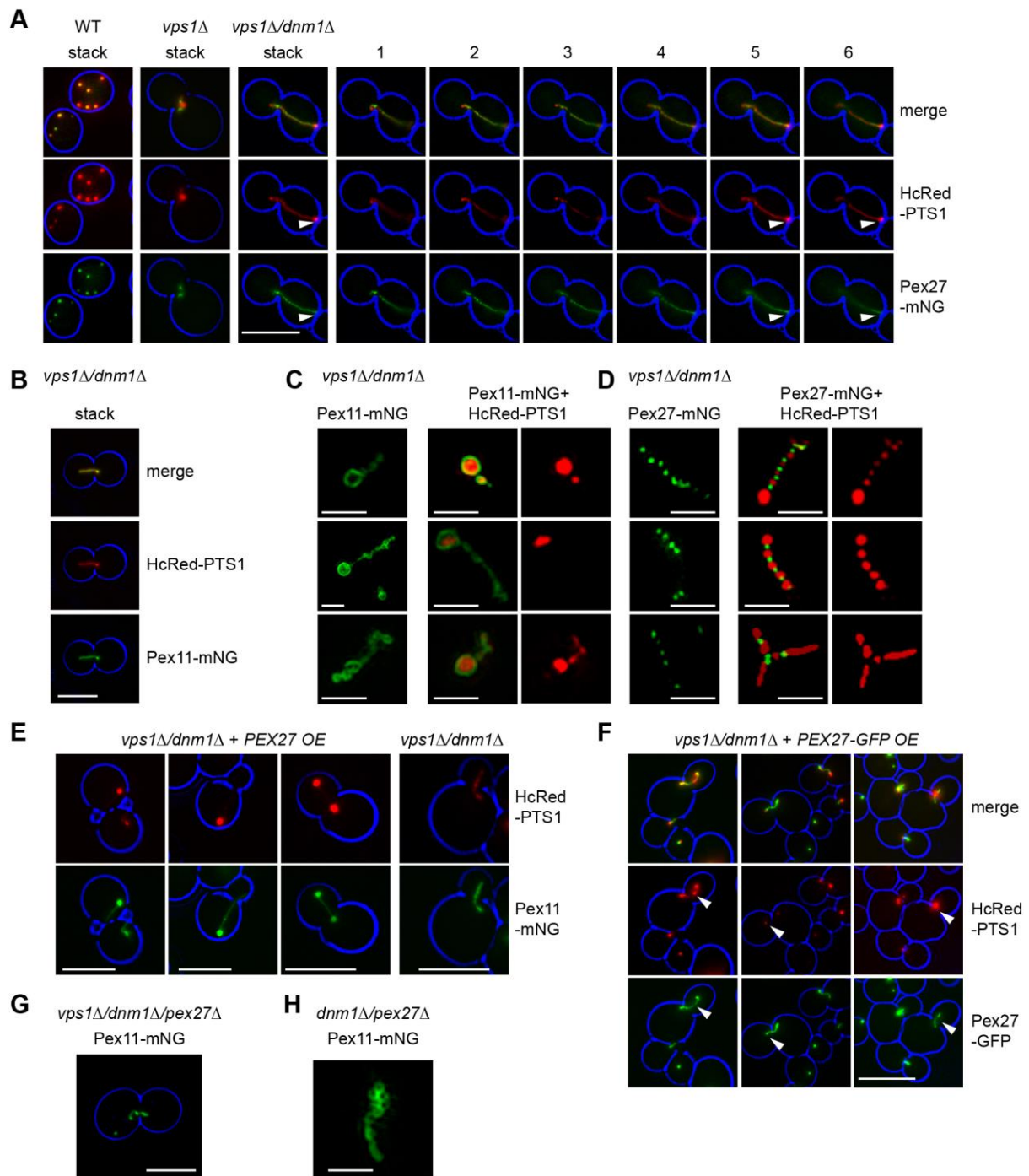
Fig. 4. Pex27-mNG is unequally distributed along the peroxisomal membrane.

(A, B) Representative epifluorescence microscopy images captured from WT, *vps1Δ* and *vps1Δ/dnm1Δ* cells co-expressing either Pex27-mNG or Pex11-mNG and HcRed-PTS1. Pex27 does not appear to label peroxisomes homogeneously in mutants with enlarged peroxisomes. Stack, represents flattened *z*-stacks, numbers 1-6 indicate individual slices 0.5 µm apart. Arrows indicate low Pex27-mNG signal

compared to HcRed-PTS1 at bulbous ends of the elongated peroxisome. Scale bar: 5 µm (B) Pex11-mNG labels peroxisomal membrane homogeneously in *vps1Δ*/*dnm1Δ* cells. Scale bar: 5 µm. (C, D) Analysis of the *vps1Δ*/*dnm1Δ* strains described in A and B with SIM. Both single labelling examples and double label examples are shown. Scale bar: 1 µm. Pex27 localises to a punctate pattern on the peroxisomal membrane, between areas enriched in matrix marker HcRed-PTS1. (E) *vps1Δ*/*dnm1Δ* cells overexpressing untagged Pex27 (*PEX27 OE*) display membrane tubules weakly labelled with matrix (HcRed-PTS1) and membrane marker (Pex11-mNG). Scale bar: 5 µm. (F) *vps1Δ*/*dnm1Δ* cells overexpressing Pex27-GFP controlled by the *TPI1* promoter (*PEX27-GFP OE*). Arrows indicate examples of HcRed-PTS1 labelled parts of elongated peroxisomes that are devoid of the Pex27-GFP label. Scale bar: 5 µm. (G/H) Pex27 is not essential for peroxisome constriction. Epifluorescence microscopy and SIM images of *vps1Δ*/*dnm1Δ/pex27Δ* and *dnm1Δ/pex27Δ* cells expressing Pex11-mNG from their endogenous locus, respectively. (G) Scale bar: 5 µm (H) Scale bar: 1 µm. (A,B,E,F,G) Cell circumference is labelled in blue. Cells were grown for extended periods in log phase on 2% glucose-containing medium.
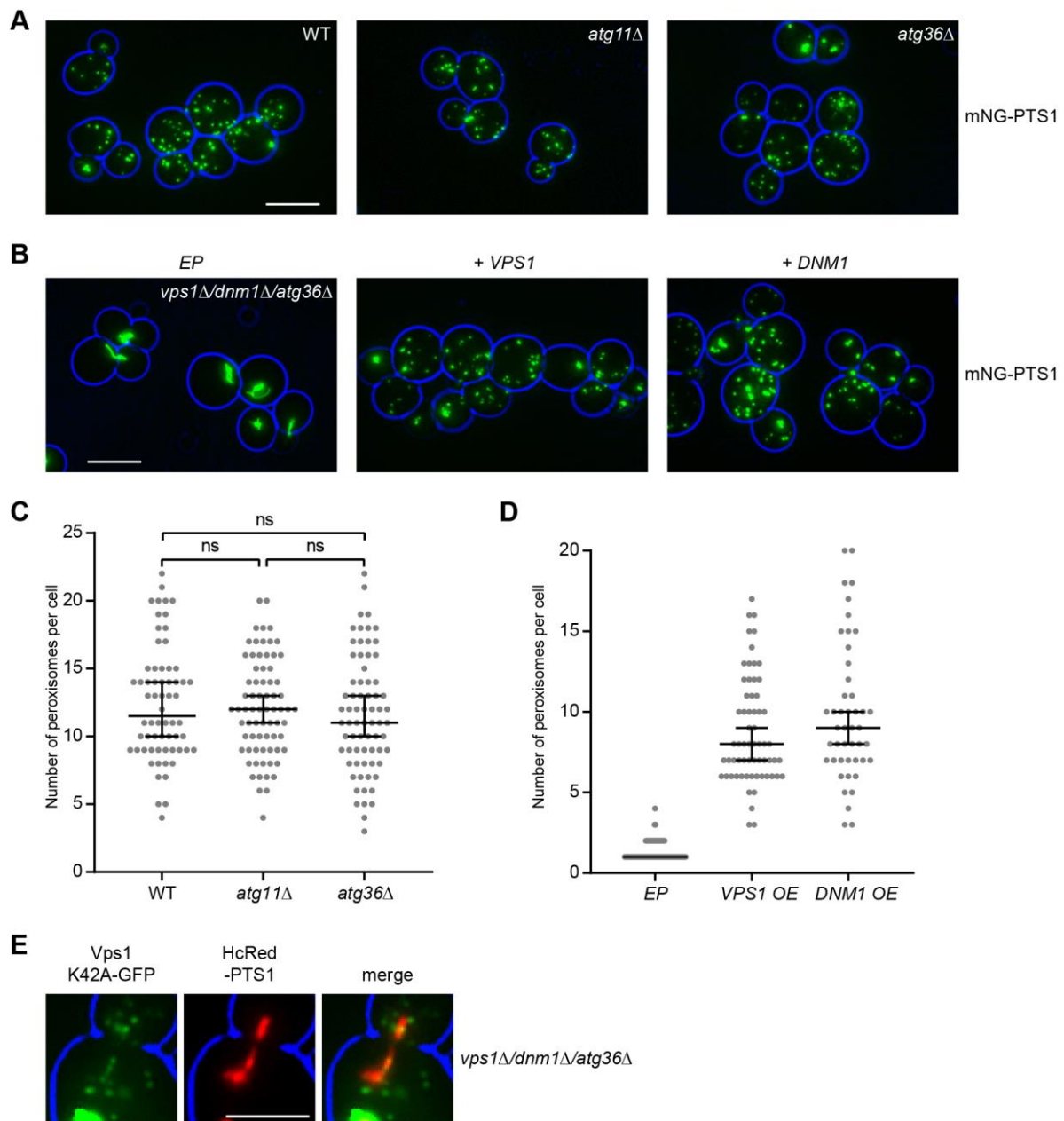
Fig. 5. Atg36 is not required for Vps1-dependent peroxisome multiplication in proliferating cells. (A, B) Representative epifluorescence microscopy images captured from WT, *atg11Δ*, *atg36Δ* and *vps1Δ*/*dnm1/atg36Δ* cells expressing mNG-PTS1 that were grown for >24h in log phase on 2% glucose-containing medium. Reintroduction of either *VPS1* or *DNM1* increases peroxisome number in *vps1Δ*/*dnm1/atg36Δ* cells. Scale bar: 5 μm. (C,D) quantitation of A and B respectively. Peroxisomes from budding cells were quantified and statistical variance Kruskal-Wallis test was employed. (E) Epifluorescence microscopy image of *vps1Δ*/*dnm1/atg36Δ* cells expressing Vps1-K42A-GFP and HcRed-PTS1. Scale bar: 2.5 μm. (A,B,E) Cell circumference is labelled in blue.
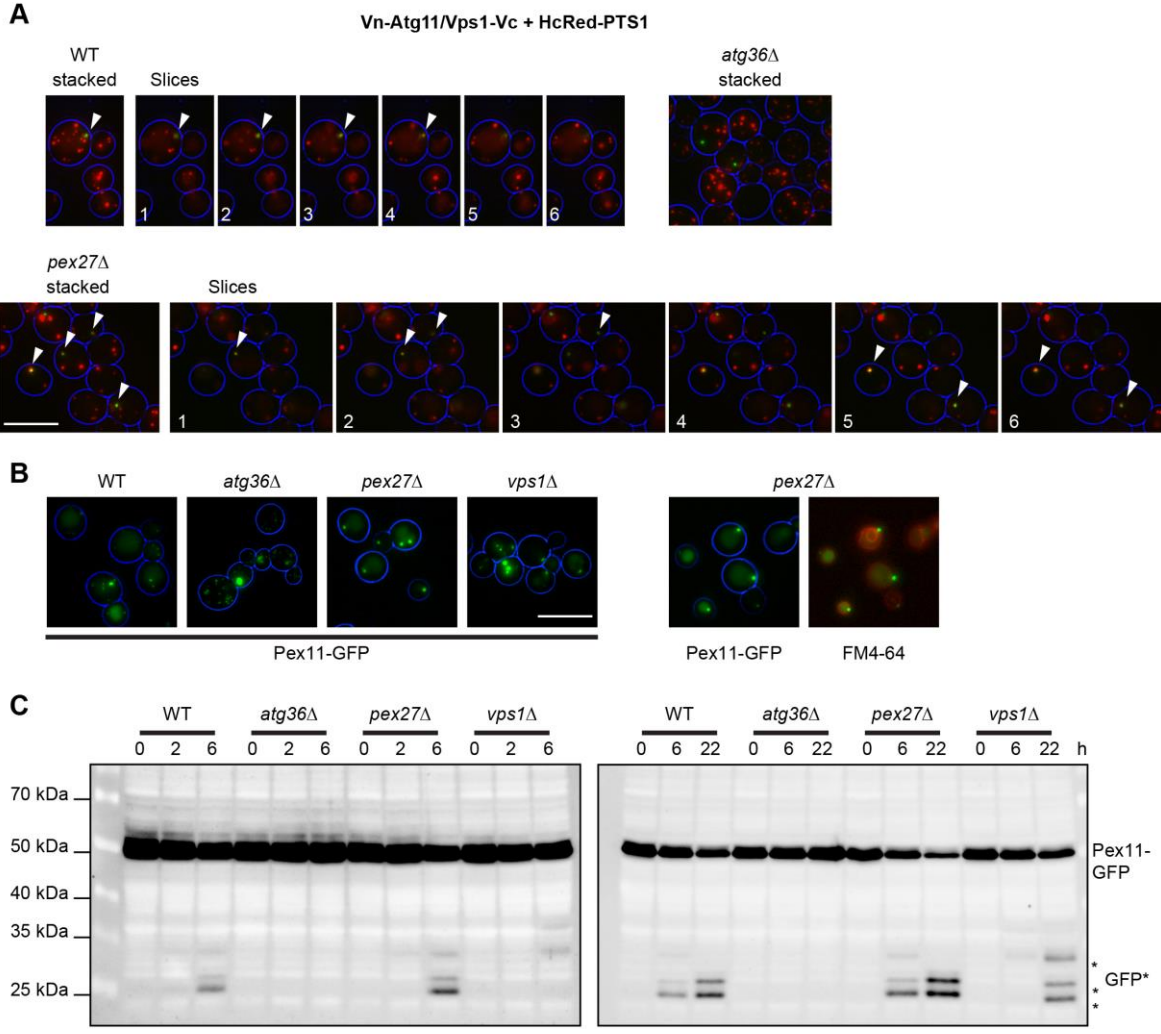
Fig. 6. Pex27 is not required for recruitment of Vps1 to the pexophagophore and efficient pexophagy. (A) Epifluorescence micrograph of bimolecular fluorescence complementation of Vn-Atg11 and Vps1-Vc in WT, *atg36Δ and pex27Δ* cells expressing HcRed-PTS1. Stack represents flattened *z*-stacks, numbers indicate individual slices, 0.5 μm apart. Cells were grown overnight on oleate medium and starved for 6 h on 2% glucose medium lacking nitrogen. (B) Representative epifluorescence microscopy images captured from WT, *atg36Δ, pex27Δ* and *vps1Δ* cells expressing Pex11-GFP. Cells were grown overnight on oleate medium and starved for 22 h on 2% glucose medium lacking nitrogen. Right hand panel, *pex27Δ* cells were subsequently stained with FM4-64 to visualise the vacuolar membrane. Scale bar: 5 μm. (A,B) Cell circumference is labelled in blue. (C) Initiation and level of pexophagy was assessed by western blot for Pex11-GFP breakdown using anti-GFP at different time points in respective mutant strains. Pexophagy was induced as in (A). * Pex11-GFP breakdown products.
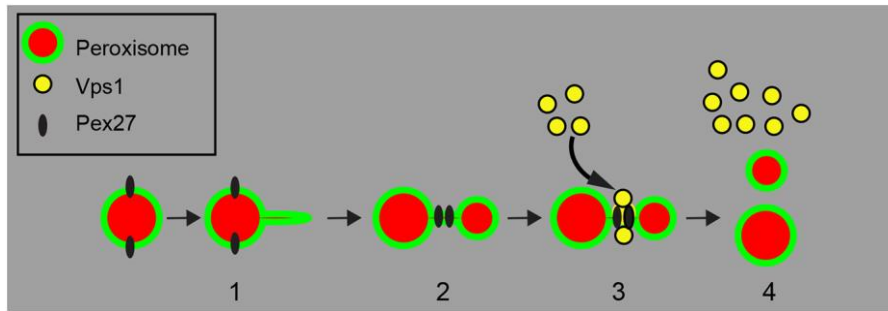
Fig. 7. Working model for the requirement of Pex25 and Pex27 in Vps1-dependent peroxisome fission. The multistep process of peroxisome fission is initiated by (1) Pex25-dependent protrusion and elongation of the peroxisomal membrane. (2) Import of proteins allows peroxisomes to grow and Pex27 concentrates on the highly curved membrane at tubular, constricted regions between bulbous areas. Vps1 associates with peroxisomes dependent on Pex27. Vps1 forms helical oligomeric assemblies around the membrane tube and GTP hydrolysis induces a conformational change and constriction of the membrane which leads to fission and Vps1 disassembly (4).
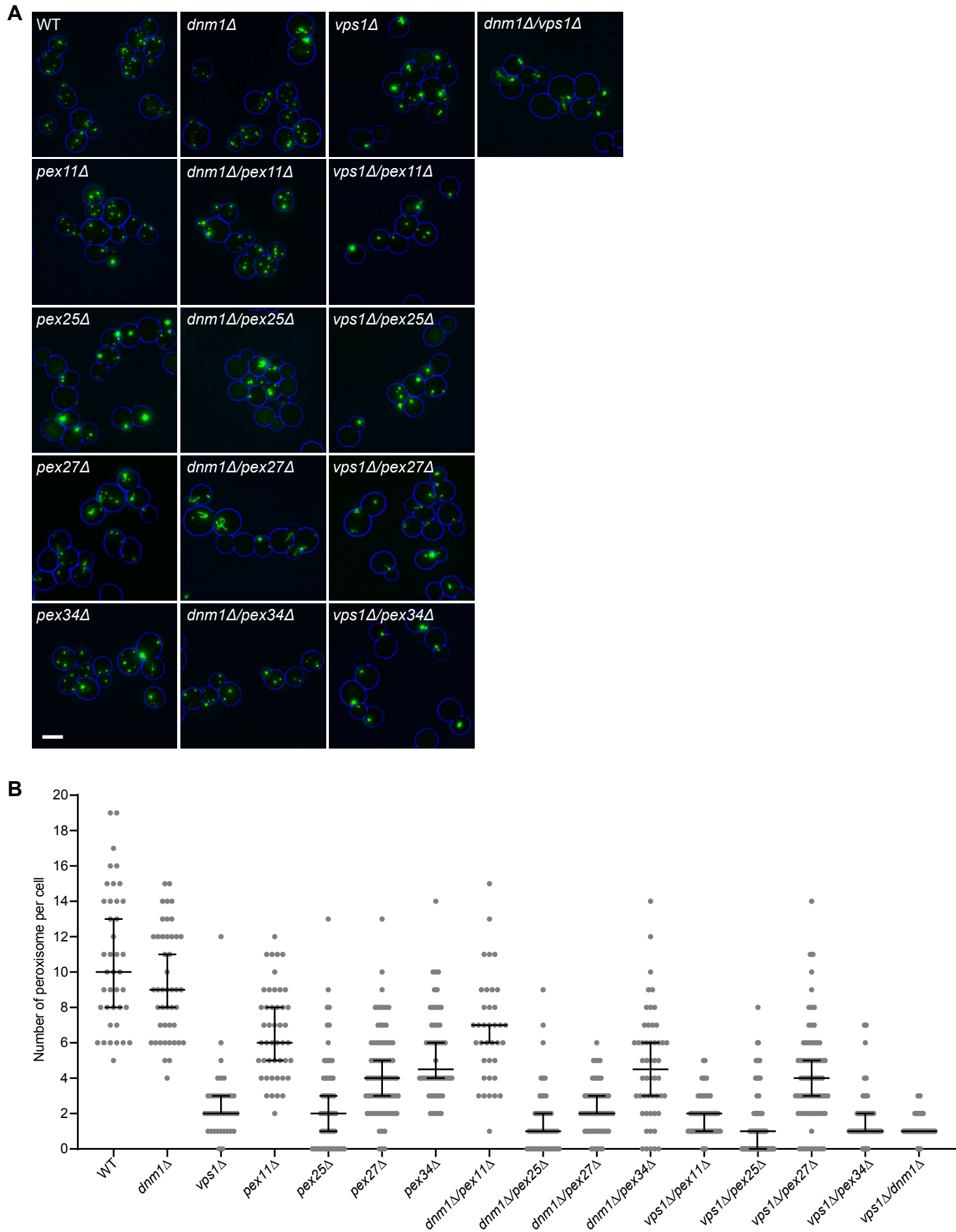
Fig. S1. Targeted screen for peroxisome multiplication: (A) Epifluorescence images captured from the various *Saccharomyces cerevisiae* mutant cells expressing mNeonGreen fluorescent protein appended with a peroxisomal targeting signal type I (mNG-PTS1). Cells were grown for an extended period on 2% glucose containing media. Representative images are shown as merged Z-stacks. Cell circumference is labelled blue. Scale bar, 5 μm. (B) Graph showing the distribution of peroxisome abundance for the strains indicated in (A). A minimum of 37 budding cells were analysed. Error bars represent the median with 95% confidence interval.
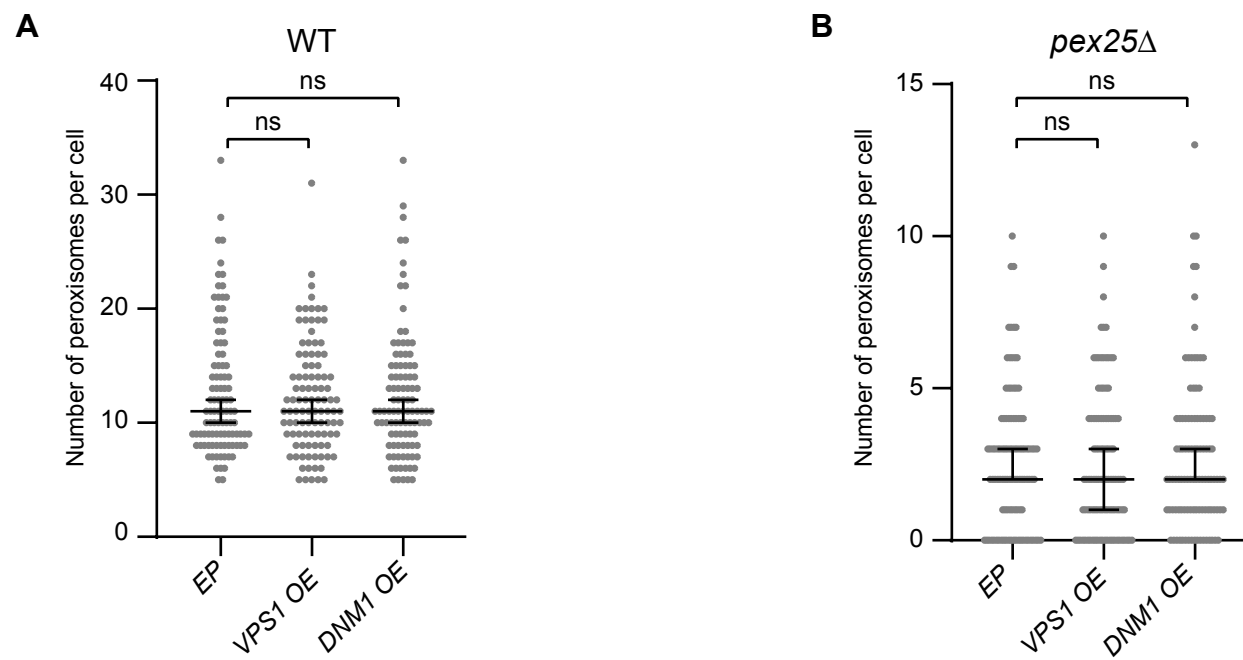
Fig. S2. *VPS1* and *DNM1* overexpression does not increase peroxisome abundance in WT and *pex25Δ* cells. WT (A) and *pex25Δ* (B) cells expressing mNG-PTS1 were transformed with either *VPS1* or *DNM1* under the control of the strong constitutive *TPI1* promoter to induce *VPS1* overexpressing (*VPS1 OE*) and *DNM1* overexpression (*DNM1 OE*) or empty plasmid as negative control (EP). Cells from exponential growing cultures were imaged using epifluorescence microscopy and the distribution of peroxisome abundance was determined. Statistical significance analysis was performed using the Kruskal-Wallis test, ns: no statistical significant difference was observed.

A WT + *EP*   WT + *PEX27 OE*   *vps1Δ* + *PEX27 OE*

HcRed-PTS1

B *vps1Δ* + Pex11-mNG

C WT + *EP*   WT + *PEX27 OE*

Pex13-GFP

D Pex11-mNG   HcRed-PTS1   merge

pex25Δ

*pex25Δ +
PEX27 OE*

E *pex25Δ* + Pex11-mNG

F Pex27-mNG   Pex11-mRFP   merge

pex25Δ

G WT   *pex25Δ*   *pex27Δ*

Pex25   45 kDa

H *vps1Δ/dnm1Δ/pex25Δ* + Pex11-GFP

EP   *PEX27 OE*

I *vps1Δ/dnm1Δ/pex25Δ* + Pex11-GFP

J *vps1Δ/dnm1Δ/pex25Δ* + *PEX27-GFP OE*

Pex27-GFP   HcRed-PTS1   merge

rare elongated peroxisome in this strain
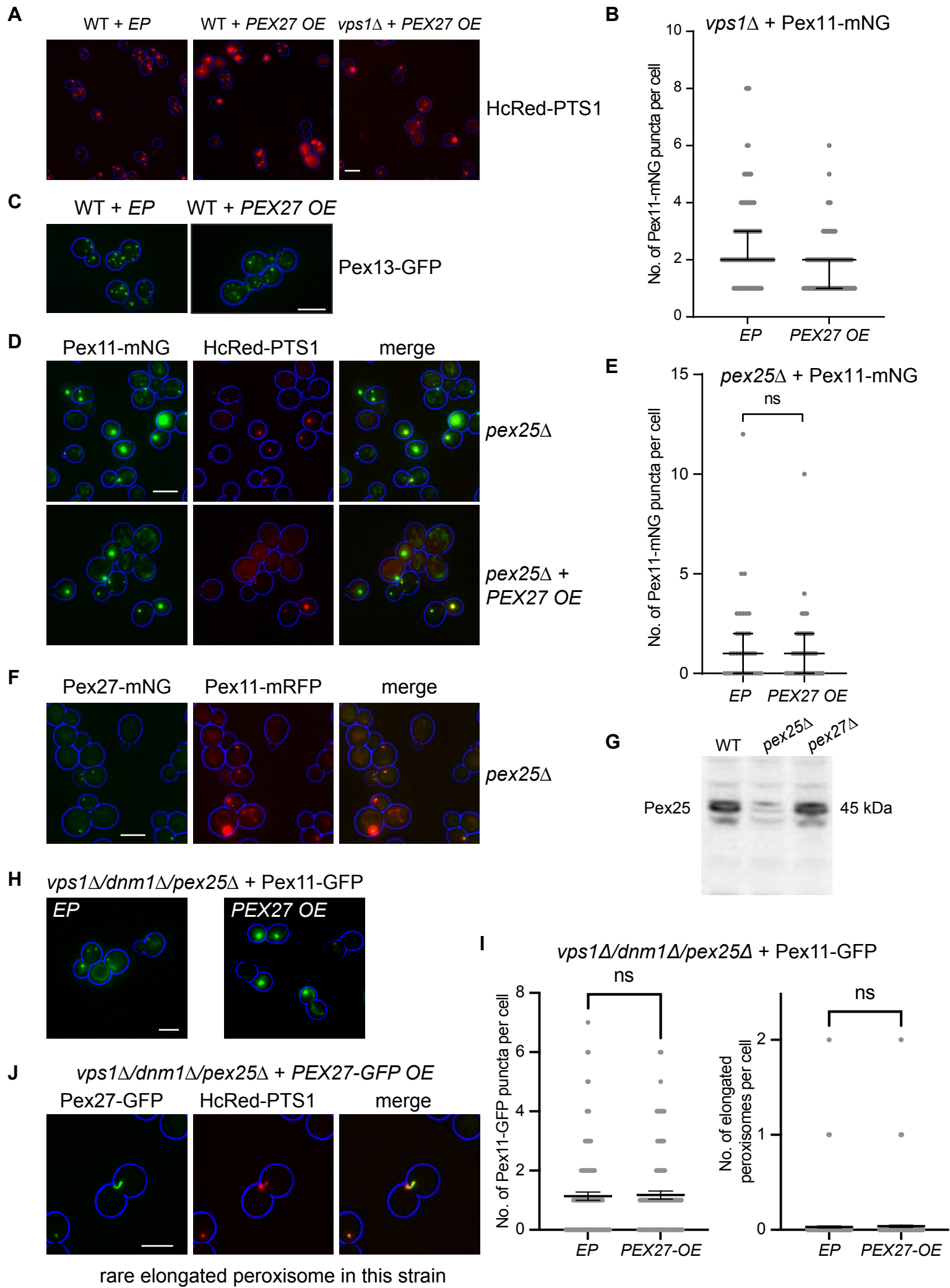
Fig. S3. *PEX27* overexpression induces multiplication of peroxisomes dependent on Vps1 and Pex25. (A) *PEX27* overexpression induces partial mislocalisation of the matrix protein marker HcRed-PTS1. WT and *vps1Δ* cells expressing HcRed-PTS1 were transformed with either an empty plasmid (EP, negative control) or *PEX27* under the control of the strong constitutive *TPI1* promoter to induce *PEX27* overexpression (*PEX27 OE*). Note partial mislocalisation of HcRed-PTS1 to cytosol in both WT and *vps1Δ* cells upon *PEX27* overexpression. (B) In *vps1Δ* cells expressing Pex11-mNG from its endogenous locus, *PEX27* overexpression does not increase mNG-labelled peroxisomal membrane structures (see also the main manuscript Fig. 2B,C). (C) *PEX27* overexpression induces an increase in Pex13-GFP labelled structures in WT cells. (D,E) Epifluorescence analysis of *pex25Δ* cells expressing Pex11-mNG from its endogenous locus and HcRed-PTS1 from a plasmid. Note how cells lacking HcRed-PTS1 puncta mislocalise Pex11-mNG to a tubular network. Overexpression of *PEX27* does not affect the Pex11-mNG labelling pattern in *pex25Δ* cells (D) or the abundance of Pex11-mNG structures (E).(F) Pex27-mNG expressed from its endogenous locus colocalises with Pex11-mRFP in *pex25Δ* cells. (G) Western blot analysis of total cellular lysates of glucose grown cells using Pex25 antiserum. Pex25 expression level is unaffected in *pex27Δ* cells. (H,I) Epifluorescence microscopy analysis of *vps1Δ/dnm1Δ/pex25Δ* cells overexpressing *PEX27*. Pex27 overexpression does not affect the Pex11-mNG labelling pattern or abundance or shape in *vps1Δ/dnm1Δ/pex25Δ* cells. Note that *PEX27* overexpression does not induce tubulation of peroxisomes in this mutant, however in less than 2% of the cells we did observe short elongated peroxisomes. See (J), (J) In the rarely elongated peroxisomes observed in *vps1Δ/dnm1Δ/pex25Δ* cells, Pex27-GFP localises to tubular parts of these peroxisomes. (B,E,I) Statistical significance analysis was performed using the Kruskal-Wallis test, ns: no statistical significant difference was observed. Cells from exponential growing cultures were used for all epifluorescence microscopy experiments. Scale bar, 5 μm. Cell circumference is labelled blue.

Table S1. Yeast strains used in this study.

Strain and genotype	Reference
BY4741 MATA his3Δ1 leu2Δ0 met15Δ0 ura3Δ0	EUROSCARF
BY4742 MATα his3Δ1 leu2Δ0 lys2Δ0 ura3Δ0	EUROSCARF
BY4742 pex11Δ::kanMX4	EUROSCARF
BY4742 pex25Δ::kanMX4	EUROSCARF
BY4742 pex27Δ::kanMX4	EUROSCARF
BY4742 pex34::his3MX6	This study
BY4742 dnm1Δ::kanMX4	EUROSCARF
BY4742 vps1Δ::kanMX4	EUROSCARF
BY4742 dnm1Δ::kanMX4 vps1Δ::his3MX6	(Motley and Hettema, 2007)
BY4742 dnm1Δ::kanMX4 pex11Δ::his3MX6	This study
BY4742 dnm1Δ::kanMX4 pex25Δ::his3MX6	This study
BY4742 dnm1Δ::kanMX4 pex27Δ::his3MX6	This study
BY4742 dnm1Δ::kanMX4 pex34Δ::his3MX6	This study
BY4742 vps1Δ::kanMX4 pex11Δ::his3MX6	This study
BY4742 vps1Δ::kanMX4 pex25Δ::his3MX6	This study
BY4742 vps1Δ::kanMX4 pex27Δ::hphMX4	This study
BY4742 vps1Δ::kanMX4 pex34Δ::his3MX6	This study
BY4742 pex27Δ::kanMX4 pex25::hphMX4	This study
BY4741 dnm1Δ::kanMX4 vps1Δ::loxp pex25 Δ::hphMX4	This study
BY4742 dnm1Δ::kanMX4 vps1Δ::loxP pex27Δ::his3MX6	This study
BY4741 pex3Δ::kanMX4	EUROSCARF
BY4741 pex3Δ::kanMX4 vps1Δ::hphMX4	(Motley and Hettema, 2007)
BY4742 dnm1Δ::kanMX4 vps1Δ::loxP PEX11::PEX11-mNG-HIS3	This study
BY4742 dnm1Δ::kanMX4 vps1Δ::loxP PEX27::PEX27-mNG-HIS3	This study
BY4741 PEX27::PEX27-TAP-HIS3	(Ghaemmaghami et al., 2003)
BY4741 atg36Δ::KanMX4	(Motley et al., 2012b)
BY4742 atg11Δ:: KanMX4	(Motley et al., 2012b)
BY4742 dnm1Δ::kanMX4 vps1Δ::loxP atg36Δ::his3MX6	This study
SEY6210 RPL7Bp-VN-ATG11::TRP1	(Mao et al., 2013)
SEY6210 RPL7Bp-VN::TRP1	(Mao et al., 2014)
SEY6210 RPL7Bp-VN-ATG11::TRP1 atg36Δ::his3MX6	This study
SEY6210 RPL7Bp-VN-ATG11::TRP1 pex27Δ::his3MX6	This study
BY4742 pex25Δ::kanMX4 PEX11::PEX11-mNG-HIS3	This study
BY4742 pex25Δ::kanMX4 PEX27::PEX27-mNG-HIS3	This study
BY4742 pex25Δ::kanMX4 TRP1::mNG-PTS1-HIS3	This study

Table S2. The plasmids used in this study.

Plasmid Name	Vector backbone	Promoter	Insert	Source
pAUL3	Ycplac33	*HIS3*	*mNG-PTS1*	Lab stock
pAUL4	Ycplac111	*HIS3*	*mNG-PTS1*	Lab stock
pLE140	Ycplac33	*PEX27*	*PEX27-ProtA*	This study
pGFP-Snc1	pRS416	*TPI1*	*GFP-Snc1*	(Lewis et al., 2000)
pAS5	Ycplac33	*HIS3*	*Hc-Red-PTS1*	Lab stock
pAS63	Ycplac111	*HIS3*	*Hc-Red-PTS1*	Lab stock
pAUL7	Ycplac111	*GAL1*	*mNG-PTS1*	Lab stock
pAUL28	Ycplac33	*HIS3*	*mKate2-PTS1*	Lab stock
pEW318	Ycplac33	-	-	Lab stock
pEW319	Ycplac111	-	-	Lab stock
pEH077	Ycplac111	*TPI1*	*3xHA-DNM1*	(Motley et al., 2008)
pEH079	Ycplac111	*TPI1*	*3xHA-VPS1*	(Motley et al., 2008)
pLE48	Ycplac111	*TPI1*	*PEX27*	This study
pKA1078	Ycplac33	*VPS1*	*VPS1-GFP*	Kathryn Ayscough
pLE141	Ycplac33	*VPS1*	*VPS1-K42A-GFP*	This study
pLE44	pFA6a	-	*mNG-HIS3*	This study
pEH012	Ycplac33	*TPI1*	*GFP-PTS1*	Lab stock
pLE41	Ycplac111	*TPI1*	*PEX27-GFP*	This study
	pRS416	*VPS1*	*VPS1-VC*	(Mao et al., 2014)
pEH007	Ycplac111	*PEX11*	*PEX11-GFP*	(Motley et al., 2012b)
pAS199	Ycplac111	*PEX11*	*PEX11-mRFP*	(Motley et al., 2015)
pEH101	Ycplac33	*PEX13*	*PEX13-GFP*	(Motley et al., 2015)